



Published in final edited form as:

Biochem Pharmacol. 2020 December ; 182: 114259. doi:10.1016/j.bcp.2020.114259.

Apigenin by targeting hnRNPA2 sensitizes triple-negative breast cancer spheroids to doxorubicin-induced apoptosis and regulates expression of *ABCC4* and *ABCG2* drug efflux transporters

Meenakshi Sudhakaran^a, Michael Ramirez Parra^b, Hayden Stoub^a, Kathleen A. Gallo^{b,*}, Andrea I. Doseff^{b,c,*}

^aPhysiology Graduate Program, Michigan State University, East Lansing, MI 48824, United States

^bDepartment of Physiology, Michigan State University, East Lansing, MI 48824, United States

^cDepartment of Pharmacology and Toxicology, Michigan State University, East Lansing, MI 48824, United States

Abstract

Acquired resistance to doxorubicin is a major hurdle in triple-negative breast cancer (TNBC) therapy, emphasizing the need to identify improved strategies. Apigenin and other structurally related dietary flavones are emerging as potential chemo-sensitizers, but their effect on three-dimensional TNBC spheroid models has not been investigated. We previously showed that apigenin associates with heterogeneous ribonuclear protein A2/B1 (hnRNPA2), an RNA-binding protein involved in mRNA and co-transcriptional regulation. However, the role of hnRNPA2 in apigenin chemo-sensitizing activity has not been investigated. Here, we show that apigenin induced apoptosis in TNBC spheroids more effectively than apigenin-glycoside, owing to higher cellular uptake. Moreover, apigenin inhibited the growth of TNBC patient-derived organoids at an *in vivo* achievable concentration. Apigenin sensitized spheroids to doxorubicin-induced DNA damage, triggering caspase-9-mediated intrinsic apoptotic pathway and caspase-3 activity. Silencing of hnRNPA2 decreased apigenin-induced sensitization to doxorubicin in spheroids by diminishing apoptosis and partly abrogated apigenin-mediated reduction of *ABCC4* and *ABCG2* efflux transporters. Together these findings provide novel insights into the critical role of hnRNPA2 in mediating apigenin-induced sensitization of TNBC spheroids to doxorubicin by increasing the expression of efflux transporters and apoptosis, underscoring the relevance of using dietary compounds as a chemotherapeutic adjuvant.

* Corresponding authors at: Department of Physiology, Department of Pharmacology & Toxicology, Michigan State University, East Lansing, MI 48824, United States (A.I. Doseff). gallok@msu.edu (K.A. Gallo), doseffan@msu.edu (A.I. Doseff).
CRediT authorship contribution statement

Meenakshi Sudhakaran: Investigation, Conceptualization, Methodology, Formal analysis, Writing - review & editing. **Michael Ramirez Parra:** Investigation, Methodology, Formal analysis. **Hayden Stoub:** Methodology. **Kathleen A. Gallo:** Conceptualization, Formal analysis, Writing - original draft, Writing - review & editing, Funding acquisition, Supervision. **Andrea I. Doseff:** Conceptualization, Formal analysis, Writing - original draft, Writing - review & editing, Funding acquisition, Supervision, Project administration.

Declaration of Competing Interest

The authors declare that they have no known competing financial interests or personal relationships that could have appeared to influence the work reported in this paper.

Keywords

Caspases; Caspase-3; Apoptosis; Dietary flavonoids; Cell death; Drug bioavailability; Breast cancer

1. Introduction

Triple-negative breast cancer (TNBC), characterized by the absence of estrogen receptor (ER), progesterone receptor (PR) and lack of amplification of human epidermal growth factor receptor 2 (HER2), is highly aggressive [1]. Its poor clinical prognosis and high mortality rates often arise from acquired resistance to first-line chemotherapeutic drugs such as doxorubicin [2]. Acquired resistance to doxorubicin is a major hurdle to effective treatment of TNBC [3], underscoring the need to identify safe and effective sensitizing agents.

Flavonoids, which are the most abundant plant phenolic compounds in human diets, are classified into different subgroups, including the flavones, based on their chemical modifications [4]. The dietary flavone apigenin, found in high levels in celery and parsley, showed increased potential as a sensitizer to doxorubicin in breast cancer (BC) cultured in two-dimensional (2D) systems [5]. However, results from 2D cell cultures have shown major shortcomings in translation to the clinic. Substantial data indicate the superiority of three-dimensional (3D) tumor spheroids as preclinical models for evaluating drug efficacy [6,7]. Thus far, the impact and underlying mechanisms of flavones on doxorubicin sensitivity in TNBC spheroids have not been investigated. Apigenin has attracted great attention due to its ability to induce apoptosis in cancer cells, by mediating caspase-9-dependent activation of the intrinsic apoptotic pathway in BC [8,9]. Apigenin is found in plants in its sugar-bound glycoside form [10]. Previous studies showed that aglycone apigenin, free of sugars, has greater anti-inflammatory activity than its glycoside counterpart in macrophages, an effect ascribed to its higher absorption [11]. However, the anti-cancer activity of apigenin aglycone and glycoside and their sensitizing capability in TNBC spheroids have not been investigated.

We recently demonstrated that apigenin associates with several proteins with varying affinities, through screening of human BC peptides using a phage-display library coupled with next generation sequencing (PD-Seq) [12]. One of the validated high affinity targets was the heterogeneous ribonuclear protein A2/B1 (hnRNPA2), an RNA binding protein involved in the regulation of mRNA stability and alternative splicing [13]. HnRNPA2 is an oncogenic driver highly upregulated in BC and correlated with poor survival [14–16]. Recent studies showed that hnRNPA2 acts as a co-transcriptional regulator [17,18]. It remains unknown, however, whether hnRNPA2 is involved in regulating apigenin-induced sensitization to doxorubicin.

Impaired apoptosis and limited drug accumulation are major causes of doxorubicin-acquired resistance [19,20]. Doxorubicin induces cell death by triggering DNA damage in the form of double-stranded breaks (DSBs), which leads to the phosphorylation of histone H2AX [21]. DNA damage stimulates the caspase-9-dependent intrinsic apoptotic pathway [22] and subsequently activates caspase-3, a central executioner of apoptosis [23,24]. Failure to

activate caspase-3 is a major contributor to the acquired resistance of cancer cells. In addition, decreased drug accumulation is recognized as a key mechanism of cancer cell multidrug resistance [25]. Drug accumulation in cells is mainly regulated by membrane-bound influx and efflux transporters [26]. The two main membrane-bound protein families responsible for doxorubicin transport in cancer cells are the ATP-binding cassette (ABC) efflux [27] and the solute carrier (SLC) influx transporters [28]. Decreased expression of the doxorubicin-selective SLC influx transporter, SLC22A16, in TNBC has been correlated to poor patient survival [29,30]. Likewise, over-expression of the ABC efflux transporters, ABCB1, ABCC1, ABCC4 and ABCG2 has been shown to contribute to doxorubicin resistance in TNBC [31–34]. Whether apigenin modulates the expression of doxorubicin-selective transporters in human TNBC spheroids has not been investigated.

In the present study, we examined the role of hnRNPA2 in regulating apigenin-mediated sensitization of human TNBC spheroids to doxorubicin. We demonstrated that hnRNPA2 plays a critical role in mediating apigenin-mediated sensitization of TNBC spheroids to doxorubicin-induced apoptosis by enhancing the activation of the intrinsic pathway and triggering caspase-3 activity. We showed that apigenin, through hnRNPA2 dependent and independent mechanisms, decreases the expression of doxorubicin-selective ABC efflux transporters. Our findings reveal a novel mechanism by which apigenin through hnRNPA2 sensitizes TNBC spheroids to doxorubicin. Together, these findings advance the concept of utilizing dietary compounds as adjuvants to overcome chemoresistance in TNBC, which may well be impactful in the treatment of other cancers.

2. Materials and methods

2.1. Chemicals

Apigenin, apigenin-7-*O*-glucoside, naringenin and doxorubicin were purchased from Sigma (St. Louis, MO). Flavonoids were dissolved in sterile dimethyl sulfoxide (DMSO, Sigma) and doxorubicin was dissolved in sterile H₂O. Growth factor reduced basement membrane Matrigel was obtained from Corning (Bedford, MA). Insulin-transferrin-selenium-X (ITS-X) and penicillin–streptomycin–glutamine solutions (PSG) were from GIBCO (Waltham, MA). Epidermal growth factor (EGF), hydrocortisone, insulin and gentamycin were purchased from Sigma. Alexa Fluor 488 conjugated cleaved caspase-3 (Asp175) (D3E9) antibody was purchased from Cell Signaling Technologies (Danvers, MA). Anti-phospho-histone γ H2AX (S139, clone JBW301) antibody was from Millipore (Billerica, MA). Anti-hnRNPA2/B1 (clone DP3B3) and anti- β -tubulin (clone AA2) antibodies were obtained from Santa Cruz Biotechnology (Santa Cruz, CA). Caspase-3 inhibitor DEVD-FMK and the caspase tetrapeptide substrates LEHD-, IETD- and DEVD-AFC were from Enzyme System Product (Livermore, CA).

2.2. 2D and 3D cell culture

MDA-MB-231 human TNBC cells (ATCC® HTB-26™) were purchased from American Type Culture Collection (ATCC, Manassas, VA) and were cultured in DMEM (GIBCO) complete media (supplemented with 5% fetal bovine serum (FBS), 100 μ g/ml streptomycin and 100 U/ml penicillin) at 37 °C and 5% CO₂. MDA-MB-231 cells were grown into

spheroids as previously described with a few modifications [35]. Briefly, MDA-MB-231 cells (passage number <20) were seeded at a density of 2000 cells/well into V-bottom 96 well plates (Greiner bio-one, #651101, Frickenhausen, Germany), centrifuged at 500 *g* for 5 min and supplemented with complete media containing 2.5% Matrigel. Spheroids were cultured for up to 6 days prior to treatments. Spheroid formation at different time points was assessed using BZ-X-800E All-in-One fluorescence microscope (Keyence, Itasca, IL). The diameters of the spheroids were determined using ImageJ software (NIH, Bethesda, MD) and growth was calculated as the difference in the diameters between the final and initial days of the treatment (diameter).

2.3. DPBA staining

Cells were incubated with the flavonoid-binding fluorescent dye diphenylboric acid 2-aminoethyl ester (DPBA; Sigma; excitation 490 nm, emission 530 nm) as previously described with a few modifications [36]. Briefly, 1×10^5 cells were grown on coverslips placed in 6-well plates (Corning) for 24 h and subsequently treated with flavonoids or DMSO for 48 h. After treatment, the cells were rinsed twice with phosphate-buffered saline (PBS, Sigma), fixed with 0.2% paraformaldehyde for 30 min at room temperature (RT) and stained with 0.2% (w/v) DPBA for 1 h at RT in the dark. After staining, the coverslips were immediately washed twice with cold PBS, mounted on slides and imaged using Olympus FluoView 1000 confocal laser scanning microscope system, configured on an Olympus IX81 inverted microscope with Olympus FluoView 1000 Advanced Software (Olympus America, Inc., Center Valley, PA). The images were processed using ImageJ and the relative fluorescence intensity was calculated as the raw integrated density per area normalized to diluent control.

2.4. Cell viability assays

For 2D cultures, cells were seeded at a density of 6×10^5 cells/ml into 96-well plates and treated with flavonoids at 50 μ M for 48 h. Cell viability was assayed with CellTiter 96 Aqueous One Solution Cell Proliferation Assay as instructed by the manufacturer (Promega, Madison, WI). In the spheroids, cell viability was determined using CellTiter-Glo[®] 3D Cell Viability Assay (Promega) following the manufacturer's instructions. The absorbance at 490 nm and luminescence for 2D culture and spheroids, respectively, were measured using Synergy[™] Neo2 Multi-Mode Microplate Reader (BioTek Instruments, Inc., Winooski, VT). The percentage of viable cells was calculated as $(Y_{\text{treatment}} - Y_{\text{blank}})/(Y_{\text{control}} - Y_{\text{blank}}) \times 100\%$, where Y is the absorbance at 490 nm or luminescence. In addition, cell viability and death were assessed by incubating spheroids with 2 μ M calcein AM (Invitrogen, Carlsbad, CA), a vital dye, and 2 μ g/mL propidium iodide (PI, Molecular Probes, Eugene, OR) for 1 h at 37 °C, as previously described [37]. After staining, spheroids were rinsed once with PBS and imaged immediately. Z-stack images of spheroids were acquired with a pitch of 40 μ m accounting for 10–15 stacks per spheroid using BZ-X-800E All-in-One fluorescence microscope. The PI mean fluorescence intensity was measured with ImageJ software.

2.5. Patient-derived xenograft (PDX) organoids

Animal studies were done in accordance with the protocols approved by the Institutional Animal Care and Use Committee at Michigan State University. PDX tumor HCI001 was

obtained from Dr. Alana Welm (Huntsman Cancer Institute, University of Utah, UT) and propagated in NSG female mice (Jackson Laboratories, Bar Harbor, ME) by serial passages. PDX organoid cultures were established as previously described [38]. PDX HCl001 fragments (5–7 mm³) were implanted into mammary fat pads of 4–5 weeks old NSG female mice and excised on reaching sizes ~2.5–3 cm³. Tumors were minced into tiny fragments and incubated in sterile digestion buffer (DMEM-F/12 supplemented with 10 mM HEPES, 2% bovine serum albumin (BSA), 5 µg/mL insulin, 0.5 µg/mL hydrocortisone, 50 µg/mL gentamycin) along with 1 mg/mL collagenase solution (Invitrogen) in a 37 °C shaking water bath at 180 rpm for 20 min. The mix was centrifuged at 500 g for 4 min and the pellet was resuspended and incubated in 10 mL of red blood cell lysing TAC buffer (170 mM Tris, pH 7.4 and 150 mM NH₄Cl, pH 7.4) at 37 °C for 2 min and immediately centrifuged. The pellet was then resuspended in DMEM-F/12 and filtered through a 100 µm cell strainer (Corning) before spinning down twice at 500 g for 40 s to remove debris. The organoid-containing pellet was diluted in modified M87 media (DMEM/F12, 2% 1FBS, 1% ITS-X, 1% PSG, 5 ng/mL EGF, 0.3 µg/mL hydrocortisone, 0.5 ng/mL cholera toxin, 5 nM 3,3',5-triiodo-L-thyronine, 0.5 nM β-estradiol, 5 µM (±)-isoproterenol hydrochloride, 50 nM ethanolamine and 50 nM *O*-phosphorylethanolamine, all from Sigma) and cultured at a density of 500/well for 5 days in ultra-low attachment 24-well dish (Corning, #3473) at 37 °C and 5% CO₂ to obtain an average diameter of 100 µm. For the treatment studies, the organoids were cultured at 100/well in modified M87 media containing 5% Matrigel. Images were processed as described in the previous section.

2.6. Immunolabeling of spheroids

Spheroids were transferred to chamber slides (Thermo Scientific, Waltham, MA) and embedded in 100% Matrigel before staining, as previously described [39]. Briefly, spheroids were fixed with 2% paraformaldehyde (Sigma) for 20 min at RT, permeabilized with 0.5% Triton X-100 for 20 min at 4 °C and washed twice with PBS. The spheroids were first incubated with primary blocking buffer (containing 0.1% BSA, 10% goat serum [Thermo Scientific], 0.2% Triton X-100, 0.05% Tween 20 in PBS) for 1 h at RT, followed by incubation with secondary blocking buffer (containing primary block with 20 µg/ml goat anti-mouse F(ab')₂ [Jackson ImmunoResearch, West Grove, PA]) for 40 min at RT. The spheroids were incubated with 0.1 µg/mL Alexa Fluor 488 conjugated cleaved caspase-3 antibody in secondary blocking buffer overnight on a gentle shaker in dark conditions at 4 °C. The spheroids were washed thrice with PBS and the nuclei were stained with 4',6-diamidino-2-phenylindole (DAPI, 5 ng/mL) for 10 min at RT. After two washes, the spheroids were mounted with coverslips using Fluoromount-G mounting media (Thermo Scientific) and allowed to dry overnight at RT in the dark prior to imaging.

2.7. Caspase activity

Protein lysates from 10 to 15 spheroids were prepared in 30 µl NP-40 lysis buffer (0.5% NP-40, 50 mM Tris, pH 7.4, 150 mM NaCl, 50 mM NaF, 10 mM Na-glycerophosphate, 5 mM Na-pyrophosphate, 1 mM orthovanadate, 1 mM DTT, 0.1 mM PMSF, and CLAP (2 µg/ml of each chymostatin, leupeptin, antipain, and pepstatin) for 30 min on ice. Caspase-9, -8 and -3 activities in cell lysates were assessed using 20 µM LEHD-, IETD- and DEVD-AFC substrates, respectively, as previously described [40]. Released AFC was

measured using a Synergy™ Neo2 Multi-Mode Microplate Reader (Filters: Ex 400 nm, Em 508 nm) and caspase activity was expressed as moles of free AFC released/minute/mg of protein.

2.8. Western blots

Cellular lysates from 0.5×10^6 cells or 10–15 spheroids were prepared as described in the above section. Equal amounts of protein were separated by SDS-PAGE, transferred onto 0.2 μ m nitrocellulose membranes (GE Amersham Biosciences, Chicago, IL), immunoblotted with antibodies, anti-phospho-histone γ H2AX, anti-hnRNPA2/B1 or anti- β -tubulin, followed by horseradish peroxidase-conjugated secondary antibodies (Thermo Scientific) and visualized by enhanced chemiluminescence (SuperSignal™ ELISA Pico Chemiluminescent Substrate, Thermo Scientific).

2.9. Kaplan–Meier plotter survival analysis

Kaplan–Meier online-plotter (<https://kmplot.com/>) was used to assess the effect of hnRNPA2 on Relapse-Free Survival (RFS) in TNBC patients [41]. Briefly, hnRNPA2 (225932_s_at) was entered into the database and RFS was selected as the survival endpoint. The analysis was restricted to ER⁻, PR⁻, HER2⁻ and basal breast cancer subtypes among the available datasets in the Kaplan–Meier database. Redundant samples and biased arrays were exempted from the analysis. Kaplan–Meier survival plots were then obtained, wherein the prognostic value was analyzed by comparing the low and high expression cohorts (upper/lower) quartiles of median gene expression.

2.10. siRNA silencing

Cells (0.5×10^6 cells/well) in a 6-well plate were transfected with 200 nM siRNA-hnRNPA2 (sense, 5′-GGAACAGUCCGUAAGCUC-3′, Dharmacon, Chicago, IL) or 200 nM siRNA-control (sense, 5′-UUCUCCGAACGUGUCACGU-3′, Qiagen, Germantown, MD) using Lipofectamine 2000 (Invitrogen, CA) for 6 h, and then diluted 2-fold in complete media and incubated for an additional 42 h. Following this first transfection, the cells were rinsed with PBS, subjected to a second round of transfection with the same amount of siRNA for 24 h, rinsed twice with PBS, and then used for spheroid formation.

2.11. RNA isolation and quantitative RT-PCR (qRT-PCR) analyses

RNA was extracted from 30 to 45 spheroids using RNeasy mini kit (Qiagen) and quality was evaluated using Synergy™ Neo2 Multi-Mode Microplate Reader. cDNA was reverse transcribed from 1 μ g RNA using the ThermoScript RT-PCR system (Invitrogen) according to the manufacturer's instructions. The qRT-PCR primer sequences used (IDT, Chicago, IL) are as follows: ABCB1: PAO-1502 (forward, 5′-TGCTCAGACAGGATGTGAGTTG-3′), PAO-1503 (reverse, 5′-AATTACAGCAAGCCTGGAACC-3′); ABCC1: PAO-1520 (forward, 5′-TGTGTGGCAACTGCATCG-3′), PAO-1521 (reverse, 5′-GTTGGTTTCCATTTTCAGATGACATCCG-3′); ABCC4: PAO-1524 (forward, 5′-GAGTTGCATGACTTGGACACGGTA-3′), PAO-1525 (reverse, 5′-AACAGAGGGTTAGCCTTCCATAAATGAGA-3′); ABCG2: PAO-1504 (forward, 5′-TATAGCTCAGATCATTGTACAGTC-3′), PAO-1505 (reverse, 5′-

GTTGGTCGTCAGGAAGAAGAG-3'); SLC22A16: PAO-1522 (forward, 5'-GCCCTCCTGAGTGGAGTGTAA-3'), PAO-1523 (reverse, 5'-TTTCATTCTCTGACTCCAGTTTTGC-3'); GAPDH: PAO-213 (forward, 5'-ACTTTGGTATCGTGGGAAGGACT-3'), PAO-214 (reverse, 5'-GTA-GAGGCAGGGATGATGTTCT-3'). Reaction mixtures in a total volume of 20 μ l containing 200 ng of cDNA template, 0.25 μ M primers and 10 μ l SYBR Green Master Mix (Applied Biosystems, Carlsbad, CA) were run in QuantStudio 3 Real-Time PCR System (Applied Biosystems) using the following conditions: 95 °C for 10 min followed by 40 cycles of 95 °C for 1 min, 60 °C for 1 min, and 72 °C for 1 min. Fold change in expression was calculated as: fold change = $2^{-\text{Ct}(\text{Apigenin})/2^{-\text{Ct}(\text{DMSO})}}$, where Ct = (Ct target – Ct internal control). All selected genes were normalized to the expression of internal control GAPDH.

2.12. Statistical analyses

All data analyses were performed using the GraphPad Prism software (San Diego, CA). Data are represented as mean \pm SEM. Statistical differences between two or more groups were determined using one-way or two-way ANOVA followed by a Tukey's post-test for multiple comparisons. For qRT-PCR results involving single groups, statistical significance was analyzed by *t*-test. Statistical significance is stated in the text.

3. Results

3.1. Differential cytotoxicity of aglycone and glycoside apigenin in human TNBC spheroids

We previously reported that apigenin aglycone has greater anti-inflammatory activity in macrophages than apigenin-7-*O*-glucoside, its sugar-bound counterpart [11], but their cytotoxic effects in human TNBC 3D models have not been investigated. To evaluate the differential effects of aglycone and glycoside apigenin (Fig. 1A) on growth and cytotoxicity in 3D human TNBC, we first established TNBC spheroids by seeding MDA-MB-231 cells for 6 days as described in Materials and Methods (Fig. 1B). On day 6, when the spheroids reached $\sim 600 \pm 15$ μ m in diameter, they were treated with 50 μ M apigenin, apigenin-7-*O*-glucoside, the flavanone naringenin or vehicle DMSO for an additional 6 days (Fig. 1B). We found that apigenin significantly diminished the spheroid growth by 85% compared with DMSO, as evidenced by the decrease in the difference in diameter between the final day 6 and initial day 0 of treatment (diameter) (Fig. 1C). Apigenin-7-*O*-glucoside had a weaker effect, reducing the spheroid growth by $\sim 40\%$. In contrast, the naringenin, a flavanone which differs structurally from apigenin by the absence of a double bond in the C ring (Fig. 1A), had only a negligible effect on TNBC spheroid growth (Fig. 1C).

To study the mechanism responsible for the effect on spheroid growth by these flavonoids, we evaluated cell viability. Spheroids treated with 50 μ M apigenin showed a $\sim 90\%$ reduction in cell viability (Fig. 1D). In contrast, apigenin-7-*O*-glucoside reduced the viability by $\sim 25\%$, while naringenin showed no significant effect on spheroid viability (Fig. 1D). Consistent with these results, a \sim six-fold increase of propidium iodide staining (PI), a marker of cell death, was observed in spheroids treated with apigenin for 6 days compared

with those treated with DMSO vehicle control (Fig. 1E and F). However, spheroids treated with apigenin-7-*O*-glucoside or naringenin showed negligible PI staining similar to that of DMSO control (Fig. 1E and F). Together these results demonstrate that apigenin aglycone has greater cytotoxic activity than its glycoside counterpart.

To investigate whether the difference in the effects of apigenin aglycone and glycoside on TNBC cell viability was due to disparities in their cellular accumulation, we quantified the intracellular levels of flavonoids by measuring the mean fluorescence intensity after staining with DPBA in MDA-MB-231 2D cultures. Cells treated with 50 μ M apigenin for 48 h showed a ~ eight -fold increase in DPBA fluorescence compared with DMSO (Fig. 1G and H), while cells treated with 50 μ M apigenin-7-*O*-glucoside or naringenin showed a subtle DPBA staining (Fig. 1G and H). Under these 2D culture conditions, apigenin reduced cell viability by 70%, similar to the levels found in 3D culture model (Fig. 1I and D, respectively). In contrast, apigenin-7-*O*-glucoside had a minor ~7% reduction in cell viability, while naringenin had no effect compared with DMSO (Fig. 1I). Collectively, these results demonstrate that aglycone apigenin is more potent than its glycoside counterpart in inducing cytotoxicity in TNBC MDA-MB-231 spheroids, which can potentially be attributed to more efficient cellular accumulation of the aglycone form.

3.2. Apigenin induces caspase-3 mediated apoptosis in spheroids

Based on the higher cytotoxic effects induced by the aglycone, we next investigated the dose response relationship of apigenin with TNBC MDA-MB-231 spheroid growth. We found that treatment with increasing concentrations of apigenin ranging from 5 to 50 μ M for 6 days reduced spheroid growth in a dose dependent manner, with significant reduction observed at concentrations as low as 5 μ M (Fig. 2A). Concomitantly, the viability of spheroids was significantly decreased in a dose-response manner at all concentrations of apigenin tested (Fig. 2B). Next, we investigated whether the reduction in cell viability is due to increased cell death. Indeed, we found a five -fold increase in cell death at concentrations as low as 5 μ M apigenin, as evidenced by a higher relative mean fluorescence intensity of PI staining, further increasing to ~seven fold in spheroids treated with 37 or 50 μ M (Fig. 2C and D). For further studies, we chose 10 μ M concentration for apigenin because of the comparable effects observed in viability and cell death among all the lowest concentrations tested. To investigate the effect of apigenin over time, we treated spheroids for 3 days with 10 μ M apigenin, which showed almost 40% reduction in growth, compared with DMSO (Fig. 2E) along a significant reduction in cell viability (Fig. 2F).

To gain further insights into the mechanisms regulating apigenin-induced cell death, we evaluated the presence of active caspase-3 in spheroids by immunostaining. Cells in the spheroid stained positive for active caspase-3 were observed upon treatment with 10 μ M apigenin for 3 days (Fig. 2G, white arrows), but remained undetectable in DMSO treated control spheroids. Consistent with these findings, caspase-3 activity increased by ~three-fold in spheroids treated for 3 days with 10 μ M apigenin (Fig. 2H) compared with DMSO, evidenced by a significant increase in AFC released during the cleavage of the caspase-3 substrate DEVD-AFC (Fig. 2H). Specificity of these results was confirmed by comparing the caspase-3 activity in spheroids treated with apigenin in the presence or absence of the

caspase-3 inhibitor DEVD-FMK. Caspase-3 activity was not observed in spheroids pretreated for 2 h with 20 μM DEVD-FMK prior to the treatment with apigenin (Fig. 2H). Collectively these data provide strong evidence that apigenin induces caspase-3-mediated apoptosis in TNBC spheroids.

3.3. Apigenin reduces the viability of TNBC human patient-derived organoids

Having shown that apigenin reduces viability in human TNBC spheroids, we next sought to investigate the effect of apigenin on human patient-derived TNBC organoids, an emerging preclinical model increasingly used in drug screening [42]. Patient-derived xenograft (PDX) organoids were generated from human TNBC PDX HCI001 tumors and cultured with increasing concentrations of apigenin or DMSO for 5 days (Fig. 3A). Notably, we found that apigenin significantly decreased organoid growth at all concentrations tested. A reduction in growth by 55% compared to DMSO was observed at 1 μM apigenin, a concentration which we previously showed to be achieved *in vivo* in mouse plasma (Fig. 3B) [11]. Apigenin also significantly reduced organoid viability. Diminution of cell viability was observed at 1 μM apigenin, although statistically insignificant, while concentrations of 5–10 μM resulted in a significant 35% decrease in viability, which reached 70% and 90% at 25 and 50 μM apigenin, respectively (Fig. 3C). Taken together, these results indicate that apigenin reduces the growth and viability of human TNBC PDX organoids at concentrations achievable *in vivo*.

3.4. Apigenin increases doxorubicin cytotoxicity in TNBC spheroids

Previous studies showed that apigenin sensitizes TNBC and ER⁺ doxorubicin resistant BC cells in 2D cultures [5]. However, the impact of apigenin on doxorubicin treatment in TNBC spheroids has not been investigated. For this purpose, we first determined the lowest concentration of doxorubicin affecting spheroid growth. Human TNBC MDA-MB-231 spheroids were cultured with different concentrations of doxorubicin ranging from 0.01 to 0.5 μM for 6 days. We found that 0.1 μM and 0.5 μM doxorubicin decreased spheroid growth over 6 days by 50% and 80%, respectively, while concentrations lower than 0.1 μM had no significant effect (Fig. 4A). Consistently, spheroid viability was significantly reduced, reaching over a 30% reduction with 0.1 μM and ~50% with 0.5 μM doxorubicin compared to DMSO (Fig. 4B). Therefore, 0.1 μM doxorubicin was selected as the dose for further experiments since it was the lowest concentration tested which reduced the growth and viability of TNBC spheroids.

To investigate whether apigenin sensitizes TNBC spheroids to doxorubicin, spheroids were treated with DMSO, 0.1 μM doxorubicin, 10 μM apigenin, or simultaneously with doxorubicin and apigenin for 3 and 6 days. Notably, the growth rate was significantly slower in spheroids treated with doxorubicin and apigenin (22 ± 4.0 $\mu\text{m}/\text{day}$) than with either of the single treatments ($\sim 36.8 \pm 3.4$ $\mu\text{m}/\text{day}$, Fig. 4C) and representing approximately a four-fold decrease compared with DMSO (79.7 ± 5.1 $\mu\text{m}/\text{day}$) (Fig. 4C).

A reduction in growth can be attributed to a decrease in cell proliferation or an increase in cell death. To study the mechanism underlying the reduction in spheroid growth observed upon doxorubicin and apigenin treatment, we evaluated the effect on cell viability and cell

death. Treatment with doxorubicin and apigenin diminished the viability by ~50% compared to spheroids treated with doxorubicin alone (Fig. 4D). In contrast, each of the single treatments reduced viability by ~25% compared to DMSO (Fig. 4D). Consistent with the significant decrease in cell viability, staining with the vital dye calcein AM (in green) was nearly undetectable in the doxorubicin and apigenin treatment, but remained evident in both of the single treatments (Fig. 4E). Likewise, PI staining, a marker indicative of cell death, increased by ~three-fold upon doxorubicin and apigenin combination treatment compared to doxorubicin alone and ~two-fold compared to apigenin alone (Fig. 4E and F). Taken together, these findings suggest that apigenin increases doxorubicin cytotoxicity by inducing cell death in human TNBC spheroids.

3.5. Apigenin-induced sensitization of TNBC spheroids to doxorubicin triggers DNA damage, activation of the intrinsic apoptotic pathway and caspase-3

To examine whether the ability of apigenin to sensitize spheroids to doxorubicin results in DNA damage, we evaluated the levels of phosphorylated H2AX (γ H2AX), a marker of double stranded breaks [21]. The levels of γ H2AX in spheroids treated with 0.1 μ M doxorubicin and 10 μ M apigenin for 6 days were significantly higher representing a 32-fold increase compared to diluent control and at least ~six-fold compared to doxorubicin alone, as indicated by western blot analyses (Fig. 5A and B). In contrast, a lower level of γ H2AX was observed with either of the single treatments, representing ~six- or twelve-fold increase in spheroid with doxorubicin or apigenin, respectively, compared to DMSO treated spheroids (Fig. 5A and B).

Next, to investigate if cell death induced by doxorubicin and apigenin combination treatment was due to the activation of the apoptotic pathways, we evaluated the activity of caspase-8 and -9, the main regulators of the extrinsic and intrinsic apoptotic pathways, respectively. We found higher caspase-9 activity in spheroids treated with doxorubicin and apigenin than either of the single treatments, as evidenced by the significant increase in the cleavage of the caspase-9-specific substrate LEHD-AFC (Fig. 5C). In contrast, caspase-8 activity was not observed in either the combination, the single treatments or DMSO control, but it was observed in spheroids treated with 20 nM tumor necrosis factor-related apoptosis-inducing ligand (TRAIL), a known inducer of the extrinsic caspase-8 mediated pathway [43], as indicated by the cleavage of the specific caspase-8 substrate IETD-AFC. These results indicate that doxorubicin and apigenin combination treatment triggers the activity of the caspase-9-mediated intrinsic apoptotic pathway. Since the activation of caspase-9 is known to trigger caspase-3 activity [44], we next investigated whether caspase-3 was induced in apigenin-mediated sensitization to doxorubicin. We found that caspase-3 activity was ~two-fold higher at day 6 in spheroids treated with the doxorubicin and apigenin than with either of the single treatments, as indicated by the increase in the cleavage of the specific caspase-3 substrate DEVD-AFC (Fig. 5E). Moreover, we found that in the presence of the inhibitor, DEVD-FMK, background caspase-3 activity, similar to DMSO controls, was found in spheroids treated with doxorubicin and apigenin combination or either of the single treatments (Fig. 5E). Taken together, these results demonstrate that apigenin-induced sensitization of TNBC spheroids to doxorubicin triggers DNA damage leading to activation of caspase-3 through the intrinsic apoptotic pathway.

3.6. Apigenin-mediated sensitization of spheroids to doxorubicin-induced apoptosis is partially dependent upon hnRNPA2

We previously showed that apigenin directly associates with hnRNPA2 in MDA-MB-231 cells [12]. However, the role of hnRNPA2 in apigenin-induced sensitization to doxorubicin has not been examined. To this end, we first evaluated the relevance of hnRNPA2 expression on relapse-free survival (RFS) in TNBC patient samples using Kaplan-Meier survival analysis as described in Material and Methods. High hnRNPA2 expression correlates with decreased RFS (log-rank $p = 0.0033$) (Fig. 6A), suggesting its relevance as a potential TNBC prognostic marker.

Based on the potentially important role of hnRNPA2 in TNBC, we next investigated whether apigenin-induced sensitization of spheroids to doxorubicin requires hnRNPA2. MDA-MB-231 cells transiently transfected with siRNA-hnRNPA2 or a scramble siRNA-control for 3 days were used to form spheroids (Fig. 6B). Silencing of hnRNPA2 was robust, as evidenced by the absence of hnRNPA2 detection in western blot analyses, which persisted throughout the 12 days of the experiment (Fig. 6B and C).

HnRNPA2 has emerged as an oncogenic driver and has been shown to promote several cancers including BC [14]. This prompted us to investigate the role of hnRNPA2 in the growth of TNBC MDA-MB-231 spheroids. We found that in the absence of hnRNPA2, the growth rate of spheroids was significantly slower at $14.6 \pm 3.0 \mu\text{m/day}$ during the first four days compared to that of siRNA-control ($54.3 \pm 0.5 \mu\text{m/day}$) (Fig. 6D). After day four, the growth rate of the spheroids lacking hnRNPA2 increased to $42.3 \pm 6.2 \mu\text{m/day}$, but the difference remained statistically significant. The overall reduction of growth rate observed in the absence of hnRNPA2 resulted in spheroids reaching diameters $\sim 482.0 \pm 13.2 \mu\text{m}$ at day 6, representing a 30% reduction compared to siRNA-controls ($\sim 681.9 \pm 19.3 \mu\text{m}$) (Fig. 6D). Together, these results demonstrate that hnRNPA2 regulates TNBC spheroid growth.

After establishing that hnRNPA2 regulates TNBC spheroid growth, we focused next on investigating the impact of hnRNPA2 on apigenin sensitization to doxorubicin-induced cell death. We found that the depletion of hnRNPA2 failed to induce cell death, as spheroids treated with vehicle DMSO showed similar background PI staining independently of hnRNPA2 silencing (Fig. 6E and F, black bars). In the presence of doxorubicin, the PI staining was similar irrespective of hnRNPA2 silencing, indicating that hnRNPA2 is dispensable for doxorubicin-induced cell death (Fig. 6E and F, green bars). In contrast, apigenin lead to a ~two-fold reduction of PI staining in spheroids lacking hnRNPA2 compared to apigenin-treated siRNA-control (Fig. 6E and 6F, blue bars), suggesting that apigenin-induced cell death depends in part on hnRNPA2. Doxorubicin and apigenin treatment in spheroids lacking hnRNPA2 resulted in a significant reduction of PI staining (~two-fold) compared with siRNA-control spheroids treated with the combination, reaching levels of PI staining similar to those observed with doxorubicin alone (Fig. 6E and 6F, red bars). Together, these results demonstrate that hnRNPA2 is dispensable for doxorubicin-induced cell death but plays a major role in apigenin-mediated sensitization to doxorubicin-induced cell death.

3.7. Apigenin decreases the expression of doxorubicin efflux transporters through hnRNPA2 dependent and independent mechanisms

Having demonstrated a role of hnRNPA2 in apigenin-mediated sensitization to doxorubicin-induced cell death, we next investigated how it impinges on the transporters of doxorubicin which play a key role in the development of acquired resistance. The influx transporter SLC22A16 and the efflux transporters ABCB1, ABCC1, ABCC4, ABCG2 have been shown to be key regulators of doxorubicin accumulation in BC cells in 2D culture models [29,31–34,45]. Thus, we first investigated whether apigenin affected those transporters by evaluating their mRNA steady state levels in human TNBC spheroids. We found that apigenin had no effect on *SLC22A16* mRNA steady state levels (Fig. 7A). In sharp contrast, apigenin significantly reduced the expression of all the doxorubicin efflux transporters tested, including *ABCB1*, *ABCC1*, *ABCC4* and *ABCG2* (Fig. 7B–E).

To assess the role of hnRNPA2 in apigenin-mediated decrease of the mRNA levels of doxorubicin efflux transporters, we evaluated their expression in spheroids lacking hnRNPA2. Spheroids generated from siRNA-control or siRNA-hnRNPA2 transfected TNBC MDA-MB-231 cells were treated with 10 μ M apigenin or DMSO for 6 days, total mRNA was isolated, and efflux transporter steady state mRNA levels were determined by qRT-PCR. We found that irrespective of hnRNPA2 silencing, apigenin reduced *ABCB1* and *ABCC1* mRNA steady state levels (Fig. 7F and G, red bars), suggesting that the effect of apigenin on these transporters is independent of hnRNPA2. However, in the absence of hnRNPA2, apigenin showed a reduced ability to decrease *ABCC4* steady state mRNA levels. When treated with apigenin, the levels of *ABCC4* steady state mRNA were 25% higher in spheroids lacking hnRNPA2 than in controls (Fig. 7H, red bars). Similarly, upon apigenin treatment, *ABCG2* mRNA steady state levels were 40% higher in spheroids lacking hnRNPA2 than in control siRNA spheroids (Fig. 7I, red bars). These findings indicate that the effect of apigenin on *ABCC4* and *ABCG2* mRNA steady state levels is partly dependent of hnRNPA2. Collectively, these results suggest that apigenin through hnRNPA2 dependent and independent mechanisms regulates the expression of doxorubicin efflux transporters in TNBC spheroids.

4. Discussion

The emergence of acquired resistance to doxorubicin is a major hurdle to successfully treating patients with TNBC [46], highlighting the need to identify new adjuvants. The use of dietary flavonoids as sensitizing agents to doxorubicin has attracted well-deserved attention due to their affordability and lack of adverse effects [47–49]. However, most of the studies have relied upon 2D culture models, which have demonstrated limited success in translation to clinical applications due to their shortcomings in mimicking the complexity of the tumor architecture. In this study, we established that the flavone apigenin targeting hnRNPA2 sensitizes TNBC spheroids to doxorubicin-induced apoptosis.

The ability of 3D cultures to better recapitulate the intricacies of tumor biology has expanded their use as powerful preclinical models for the screening of potential new therapeutics [6,42]. However, until now, only a few studies have used 3D culture models to evaluate the physiological activity of flavonoids. Recently, the flavones apigenin and luteolin

have been shown to suppress intravasation through the endothelial barrier of MDA-MB-231 and ER⁺ MCF-7 BC spheroids, supporting their anti-metastatic activity [50]. A few other studies available so far using colorectal, prostate and BC spheroids, showed that the flavonoids resveratrol, epigallocatechin gallate and quercetin decrease growth and induce apoptosis [51–53]. Our results herein demonstrate that apigenin aglycone reduced the growth and viability of human TNBC MDA-MB-231 spheroids more effectively than its glucoside counterpart apigenin-7-*O*-glucoside (Fig. 1C–F), which is likely due to the higher cellular absorption of the aglycone (Fig. 1G and H). In agreement with our observations, studies found that apigenin is Caco-2 colorectal adenocarcinoma cells are five-times more permeable to apigenin than to apigenin-7-*O*-glucoside [54]. Previous studies in macrophages showed higher cellular accumulation of apigenin than its glycoside, which could attribute to the higher anti-inflammatory activity of the aglycone [11]. Our findings are also in agreement with studies showing that other aglycones including, baicalein, wogonin and genistein have higher anti-proliferative activity than their glycosides in ER⁺ MCF-7 BC in 2D culture models [55,56]. In addition, the flavone luteolin induces apoptosis more effectively its glycoside in MDA-MB-231 2D culture systems [55], but whether this difference is due to disparities in absorption was not tested. The limited activity of apigenin-7-*O*-glucoside and naringenin in spheroid growth and viability (Fig. 1C–F) was accompanied by their low cellular accumulation (Fig. 1G–I). These differences in cellular accumulation may be attributed to the planar structure of apigenin aglycone, which is conferred by the presence of a double bond between carbon 2 and 3 on the C ring. This planar structure contrasts with the non-planar structure of naringenin, which lacks the double bond, or the change in the conformation of the structure due to the addition of the sugar in apigenin-7-*O*-glucoside. Highlighting the impact of the structure on bioavailability *in vivo*, our previous studies showed that glycosylation reduced intestinal absorption of apigenin into systemic circulation in mice fed with celery-derived apigenin rich foods [11]. Together, our results show different biological efficacy of aglycone and glycoside apigenin in TNBC spheroid growth and viability, highlighting the impact that the structure of flavonoids plays in determining their biological activity.

In our investigation of the mechanism by which apigenin reduces the viability of MDA-MB-231 spheroids, we found that apigenin induced caspase-3 activity, supporting its ability to induce apoptosis (Fig. 2G and H). Our results agree with previous observations that apigenin induced caspase-3 activity in 2D cultures of TNBC and BC cells [8,9]. Our studies also showed that apigenin reduced the growth and viability of human TNBC PDX organoids at a concentration as low as 1 μ M (Fig. 2). This observation is important, because we previously showed that this biological active concentration is readily achieved *in vivo* in the plasma of mice fed with celery-derived foods rich in apigenin [11], and was sufficient to reduce inflammation [57]. Our present findings highlight the potential of using diets rich in apigenin to deliver bioactive concentrations of this flavonoid to induce TNBC cell death.

Only a couple of studies to date have evaluated the activity of flavonoids as sensitizers to doxorubicin in spheroid models. For instance, the flavonol resveratrol, found in grapes, and the flavone chrysin, abundant in honey, increased the intracellular accumulation of doxorubicin in pancreatic and lung cancer spheroids, respectively [58,59]. While the mechanisms associated to resveratrol have not been investigated so far, chrysin was found to

decrease the expression of the tight junction proteins claudin-1 and 11, increasing transepithelial fluxes but had no effect in ABC transporters [59]. Supporting the relevance of 3D culture models, chrysin-mediated increased doxorubicin cytotoxicity was exclusively observed in 3D culture models but was completely ineffective in 2D culture systems [59]. Herein, we found that apigenin increased doxorubicin cytotoxicity by promoting cell death (Figs. 4 and 8). So far, the only studies done using showed hepatocellular carcinoma xenograft models showed that apigenin in combination with doxorubicin suppressed growth and induced apoptosis [49]. Together our findings warrant future studies using TNBC animal models. Our studies showed that apigenin and doxorubicin treatment triggered DNA damage (Fig. 5A and B), leading to the activation of caspase-9 and -3 (Fig. 5C–E). We previously showed that apigenin induced DNA damage increasing γ H2AX and promoting cell cycle arrest in myeloid leukemia [47]. Our results also agree with previous observations that apigenin enhanced doxorubicin-induced cytotoxicity through caspase-9 and 3 activity in 2D cultures of leukemia, MCF-7 and hepatocellular carcinoma cancer cell lines [5,47,60]. We and others have previously reported that apigenin modulates proteins such as ATM, PKC, p21, Bcl-2, Bax involved in DNA damage and apoptotic signalling pathways [8,61] in different cancer cell lines, further supporting the ability of apigenin to halting tumor cell proliferation mechanisms. No increase in caspase-8 activity was observed in our studies, indicating a lack of involvement of the extrinsic pathways (Fig. 5D and 8). In contrast, enhanced caspase-8 activity in MDA-MB-231 2D cell cultures treated with doxorubicin and apigenin was previously reported [8,62]. These discrepancies may owe to the differences in the concentrations and culture conditions, emphasizing the disparities between 2D and 3D models in delivering results that could be recapitulated *in vivo*.

Apigenin has been reported to possess anticancer effects both *in vitro* and *in vivo* by modulating a broad range of molecular signaling pathways involved in tumor proliferation and inhibition of apoptosis [63], whether these proteins are directly targeted by apigenin however remains unlikely. Thus our findings present evidence that apigenin through direct targeting to hnRNPA2 contributes to the modulation of doxorubicin transporters. To better understand the mechanisms responsible for these effects of apigenin, we previously identified proteins that associate directly with apigenin [12]. Our studies demonstrated that apigenin associates with a high affinity to the RNA binding protein hnRNPA2 [12]. HnRNPA2 has been identified as a potential prognostic marker in several cancers including glioblastoma, lung and colorectal cancers [64–67]. High hnRNPA2 protein levels have been detected in brush lung cancer biopsies, supporting its role as an early detection marker [68]. Here, we show using Kaplan Meier survival analysis that high hnRNPA2 expression correlates with decreased RFS (Fig. 6A), supporting the relevance of hnRNPA2 as a potential prognostic marker for TNBC recurrence. A previous study reported that hnRNPA2 did not impact the overall survival rate of TNBC patients [69]. One may speculate that this lack of impact may owe to the choice of datasets in the analyses. Our studies used all the 35 available breast cancer-specific datasets (see Material and Methods), unfortunately, no information regarding the same was provided in the previous study [69]. In this study, we found that hnRNPA2 is critical for human TNBC spheroid growth (Fig. 6D). Our results are in agreement with previous studies showing that hnRNPA2 plays a critical role in TNBC tumor growth in xenografts models [14,69]. Our results further demonstrate that hnRNPA2

is central for apigenin-induced TNBC spheroid death, whereas it is dispensable for doxorubicin-induced death (Fig. 6E, 6F and 8). We previously reported that apigenin modulates the splicing patterns of several hnRNPA2 target mRNAs including caspase-9 [12]. Whether hnRNPA2 is required for apigenin-mediated perturbations in the splicing of mRNA transcripts encoding apoptotic molecules in TNBC spheroids requires further investigation.

Identification of the critical role of hnRNPA2 in apigenin-induced apoptosis prompted us to investigate its ability to regulate the levels of drug transporters, which are known to diminish doxorubicin efficacy by decreasing drug availability. Previous studies established that apigenin reduces the expression of drug efflux transporters *ABCB1*, *ABCC1*, and *ABCG2* in ER + MCF7 cells in 2D cultures [5], which were confirmed in our 3D TNBC spheroid model (Fig. 7B, C and E). In addition, we found that apigenin also reduced the expression of the efflux transporter *ABCC4* (Fig. 7D), but has no effect on the *SLC22A16* doxorubicin influx transporter (Fig. 7A and 8). Mechanistically, we demonstrated that hnRNPA2 is required for apigenin-mediated reduction of *ABCC4* and *ABCG2* mRNA expression in TNBC spheroids (Fig. 7H, 7I and 8). In contrast, our data indicate that apigenin-induced reduction of *ABCB1* and *ABCC1* expression levels is independent of hnRNPA2 (Fig. 7F, 7G and 8). The reasons for the differences in the dependence ABC transporter regulation on hnRNPA2 are yet to be elucidated. Recent studies have shown that in addition to its splicing activities, hnRNPA2 is a co-regulator of transcription factors including hypoxia inducing factor (HIF)-1 α and nuclear factor kappa-light-chain-enhancer of activated B cells (NF- κ B) [17,18,70]. Thus, it is provocative to speculate that hnRNPA2 may regulate *ABCC4* and *ABCG2* expression through its association with transcription factors. In support of this hypothesis, hnRNPA2 was found to stabilize *HIF-1 α* [71], leading to enhanced binding of HIF-1 α to the hypoxia response element located in the *ABCG2* promoter [70]. Moreover, NF- κ B binding to the *ABCG2* promoter contributed to the upregulation of their mRNA and protein expression in MCF-7 cells [72]. In addition, apigenin was found to reduce HIF-1 α protein levels in MDA-MB-231 cells [73] and the transcriptional activity of NF- κ B in ER⁺ and HER2⁺ BC cells [74]. Thus, it is conceivable that apigenin reduces *ABCG2* mRNA expression through the downregulation of NF- κ B transcriptional activity. Our findings herein which have uncovered the role of hnRNPA2 in apigenin-induced regulation of doxorubicin transporters, open the door to these warranted future studies.

In conclusion, hnRNPA2 plays a critical role in mediating apigenin-mediated sensitization of TNBC spheroids to doxorubicin-induced apoptosis and is partially responsible for regulating the expression of doxorubicin-selective efflux transporters. These findings provide novel insights into the mechanisms underlying the potency of apigenin as a sensitizer to doxorubicin, underscoring the potential impactful relationship between apigenin rich diets and chemotherapeutic drugs that may provide a strategy to improve chemotherapy response in cancers beyond TNBC.

Acknowledgements

We thank Dr. A. Welm for the human TNBC PDX HCI001 tumor and Dr. R. Das for the NSG mice. We thank Dr. S. O'Reilly for technical assistance with mouse surgeries, E. Miller for assistance with organoid preparation and cell culture and A. Gjidoda with the preparation of the figures. The work was supported by grant USDA-AFRI-2018-03994, NSF-IOE-1733633, USDA-AFRI-2020-67017-30838, and MSU general funds to A.I.D; DoD

BCRP W81XWH-15-1-0018 and a METAvivor Research Award to K.A.G. M. S. was supported by a graduate research fellowship support from the Plant Biotechnology for Health and Sustainability Training Program Project NIH T32-GM110523.

References

- [1]. Andre F, Pusztai L, Molecular classification of breast cancer: implications for selection of adjuvant chemotherapy, *Nat. Clin. Pract. Oncol* 3 (11) (2006) 621–632. [PubMed: 17080180]
- [2]. Lin NU, Vanderplas A, Hughes ME, Theriault RL, Edge SB, Wong YN, Blayney DW, Niland JC, Winer EP, Weeks JC, Clinicopathologic features, patterns of recurrence, and survival among women with triple-negative breast cancer in the National Comprehensive Cancer Network, *Cancer* 118 (22) (2012) 5463–5472. [PubMed: 22544643]
- [3]. Echeverria GV, Ge Z, Seth S, Zhang X, Jeter-Jones S, Zhou X, Cai S, Tu Y, McCoy A, Peoples M, Sun Y, Qiu H, Chang Q, Bristow C, Carugo A, Shao J, Ma X, Harris A, Mundi P, Lau R, Ramamoorthy V, Wu Y, Alvarez MJ, Califano A, Moulder SL, Symmans WF, Marszalek JR, Heffernan TP, Chang JT, Piwnica-Worms H, Resistance to neoadjuvant chemotherapy in triple-negative breast cancer mediated by a reversible drug-tolerant state, *Sci. Transl. Med* 11 (488) (2019).
- [4]. Sudhakaran M, Sardesai S, Doseff AI, Flavonoids, New frontier for immuno-regulation and breast cancer control, *Antioxidants (Basel)* 8 (4) (2019).
- [5]. Seo HS, Ku JM, Choi HS, Woo JK, Lee BH, Kim DS, Song HJ, Jang BH, Shin YC, Ko SG, Apigenin overcomes drug resistance by blocking the signal transducer and activator of transcription 3 signaling in breast cancer cells, *Oncol. Rep* 38 (2) (2017) 715–724. [PubMed: 28656316]
- [6]. Vidi PA, Bissell MJ, Lelievre SA, Three-dimensional culture of human breast epithelial cells: the how and the why, *Methods Mol. Biol* 945 (2013) 193–219. [PubMed: 23097109]
- [7]. Xu R, Boudreau A, Bissell MJ, Tissue architecture and function: dynamic reciprocity via extra- and intra-cellular matrices, *Cancer Metastasis Rev* 28 (1–2) (2009) 167–176. [PubMed: 19160017]
- [8]. Choi EJ, Kim G-H, Apigenin induces apoptosis through a mitochondria/caspase-pathway in human breast cancer MDA-MB-453 cells, *J. Clin. Biochem. Nutr* 44 (3) (2009) 260–265. [PubMed: 19430615]
- [9]. Seo HS, Ku JM, Choi HS, Woo JK, Jang BH, Go H, Shin YC, Ko SG, Apigenin induces caspase-dependent apoptosis by inhibiting signal transducer and activator of transcription 3 signaling in HER2-overexpressing SKBR3 breast cancer cells, *Mol. Med. Rep* 12 (2) (2015) 2977–2984. [PubMed: 25936427]
- [10]. Jiang N, Doseff AI, Grotewold E, Flavones: from biosynthesis to health benefits, *Plants (Basel, Switzerland)* 5 (2) (2016) 27.
- [11]. Hostetler G, Riedl K, Cardenas H, Diosa-Toro M, Arango D, Schwartz S, Doseff AI, Flavone deglycosylation increases their anti-inflammatory activity and absorption, *Mol. Nutr. Food Res* 56 (4) (2012) 558–569. [PubMed: 22351119]
- [12]. Arango D, Morohashi K, Yilmaz A, Kuramochi K, Parihar A, Brahimaj B, Grotewold E, Doseff AI, Molecular basis for the action of a dietary flavonoid revealed by the comprehensive identification of apigenin human targets, *Proc. Natl. Acad. Sci. U.S.A* 110 (24) (2013) E2153–E2162. [PubMed: 23697369]
- [13]. Glisovic T, Bachorik JL, Yong J, Dreyfuss G, RNA-binding proteins and post-transcriptional gene regulation, *FEBS Lett* 582 (14) (2008) 1977–1986. [PubMed: 18342629]
- [14]. Hu Y, Sun Z, Deng J, Hu B, Yan W, Wei H, Jiang J, Splicing factor hnRNPA2B1 contributes to tumorigenic potential of breast cancer cells through STAT3 and ERK1/2 signaling pathway, *Tumour Biol* 39 (3) (2017).
- [15]. Zhou J, Allred DC, Avis I, Martinez A, Vos MD, Smith L, Treston AM, Mulshine JL, Differential expression of the early lung cancer detection marker, heterogeneous nuclear ribonucleoprotein-A2/B1 (hnRNP-A2/B1) in normal breast and neoplastic breast cancer, *Breast Cancer Res. Treat* 66 (3) (2001) 217–224. [PubMed: 11510693]

- [16]. Klinge CM, Piell KM, Tooley CS, Rouchka EC, HNRNPA2/B1 is upregulated in endocrine-resistant LCC9 breast cancer cells and alters the miRNA transcriptome when overexpressed in MCF-7 cells, *Sci. Rep* 9 (1) (2019) 9430. [PubMed: 31263129]
- [17]. Guha M, Pan H, Fang JK, Avadhani NG, Heterogeneous nuclear ribonucleoprotein A2 is a common transcriptional coactivator in the nuclear transcription response to mitochondrial respiratory stress, *Mol. Biol. Cell* 20 (18) (2009) 4107–4119. [PubMed: 19641020]
- [18]. Xuan Y, Wang J, Ban L, Lu JJ, Yi C, Li Z, Yu W, Li M, Xu T, Yang W, Tang Z, Tang R, Xiao X, Meng S, Chen Y, Liu Q, Huang W, Guo W, Cui X, Deng W, hnRNP A2/B1 activates cyclooxygenase-2 and promotes tumor growth in human lung cancers, *Mol. Oncol* 10 (4) (2016) 610–624. [PubMed: 26774881]
- [19]. Inao T, Iida Y, Moritani T, Okimoto T, Tanino R, Kotani H, Harada M, Bcl-2 inhibition sensitizes triple-negative human breast cancer cells to doxorubicin, *Oncotarget* 9 (39) (2018) 25545–25556. [PubMed: 29876007]
- [20]. Taylor CW, Dalton WS, Parrish PR, Gleason MC, Bellamy WT, Thompson FH, Roe DJ, Trent JM, Different mechanisms of decreased drug accumulation in doxorubicin and mitoxantrone resistant variants of the MCF7 human breast cancer cell line, *Br. J. Cancer* 63 (6) (1991) 923–929. [PubMed: 1676902]
- [21]. Rogakou EP, Pilch DR, Orr AH, Ivanova VS, Bonner WM, DNA double-stranded breaks induce histone H2AX phosphorylation on serine 139, *J. Biol. Chem* 273 (10) (1998) 5858–5868. [PubMed: 9488723]
- [22]. Norbury CJ, Zhivotovsky B, DNA damage-induced apoptosis, *Oncogene* 23 (16) (2004) 2797–2808. [PubMed: 15077143]
- [23]. Yang XH, Sladek TL, Liu X, Butler BR, Froelich CJ, Thor AD, Reconstitution of caspase 3 sensitizes MCF-7 breast cancer cells to doxorubicin- and etoposide-induced apoptosis, *Cancer Res* 61 (1) (2001) 348–354. [PubMed: 11196185]
- [24]. Cohen GM, Caspases: the executioners of apoptosis, *Biochem. J* 326 (Pt 1)(Pt 1) (1997) 1–16. [PubMed: 9337844]
- [25]. Hembruff SL, Laberge ML, Villeneuve DJ, Guo B, Veitch Z, Cecchetto M, Parissenti AM, Role of drug transporters and drug accumulation in the temporal acquisition of drug resistance, *BMC Cancer* 8 (1) (2008) 318. [PubMed: 18980695]
- [26]. Giacomini KM, Huang S-M, Tweedie DJ, Benet LZ, Brouwer KLR, Chu X, Dahlin A, Evers R, Fischer V, Hillgren KM, Hoffmaster KA, Ishikawa T, Keppler D, Kim RB, Lee CA, Niemi M, Polli JW, Sugiyama Y, Swaan PW, Ware JA, Wright SH, Wah Yee S, Zamek-Gliszczynski MJ, Zhang L, C. The International Transporter, Membrane transporters in drug development, *Nat. Rev. Drug Discovery* 9 (3) (2010) 215–236. [PubMed: 20190787]
- [27]. Gottesman MM, Fojo T, Bates SE, Multidrug resistance in cancer: role of ATP-dependent transporters, *Nat. Rev. Cancer* 2 (1) (2002) 48–58. [PubMed: 11902585]
- [28]. Hediger MA, Romero MF, Peng J-B, Rolfs A, Takanaga H, Bruford EA, The ABCs of solute carriers: physiological, pathological and therapeutic implications of human membrane transport proteins, *Pflügers Archiv* 447 (5) (2004) 465–468. [PubMed: 14624363]
- [29]. Okabe M, Unno M, Harigae H, Kaku M, Okitsu Y, Sasaki T, Mizoi T, Shiiba K, Takanaga H, Terasaki T, Matsuno S, Sasaki I, Ito S, Abe T, Characterization of the organic cation transporter SLC22A16: a doxorubicin importer, *Biochem. Biophys. Res. Commun* 333 (3) (2005) 754–762. [PubMed: 15963465]
- [30]. Wu J, Hu S, Chen Y, Li Z, Zhang J, Yuan H, Shi Q, Shao N, Ying X, BCIP: a gene-centered platform for identifying potential regulatory genes in breast cancer, *Sci. Rep* 7 (1) (2017) 45235. [PubMed: 28327601]
- [31]. Bao L, Hazari S, Mehra S, Kaushal D, Moroz K, Dash S, Increased expression of P-glycoprotein and doxorubicin chemoresistance of metastatic breast cancer is regulated by miR-298, *Am. J. Pathol* 180 (6) (2012) 2490–2503. [PubMed: 22521303]
- [32]. Gao M, Miao L, Liu M, Li C, Yu C, Yan H, Yin Y, Wang Y, Qi X, Ren J, miR-145 sensitizes breast cancer to doxorubicin by targeting multidrug resistance-associated protein-1, *Oncotarget* 7 (37) (2016) 59714–59726. [PubMed: 27487127]

- [33]. Kochel TJ, Reader JC, Ma X, Kundu N, Fulton AM, Multiple drug resistance-associated protein (MRP4) exports prostaglandin E2 (PGE2) and contributes to metastasis in basal/triple negative breast cancer, *Oncotarget* 8 (4) (2017) 6540. [PubMed: 28029661]
- [34]. Britton KM, Eyre R, Harvey JJ, Stemke-Hale K, Browell D, Lennard TWJ, Meeson AP, Breast cancer, side population cells and ABCG2 expression, *Cancer Lett* 323 (1) (2012) 97–105. [PubMed: 22521545]
- [35]. Ye J, Liu Y, Xia X, Meng L, Dong W, Wang R, Fu Z, Liu H, Han R, Improved safety and efficacy of a lipid emulsion loaded with a paclitaxel-cholesterol complex for the treatment of breast tumors, *Oncol Rep* 36 (1) (2016) 399–409. [PubMed: 27175803]
- [36]. Grootaert C, Gonzales GB, Vissenaekens H, Van de Wiele T, Raes K, Smagghe G, Van Camp J, Flow cytometric method for the detection of flavonoids in cell lines, *J. Biomol. Screen* 21 (8) (2016) 858–865. [PubMed: 27280551]
- [37]. Vargo MA, Voss OH, Poustka F, Cardounel AJ, Grotewold E, Doseff AI, Apigenin-induced-apoptosis is mediated by the activation of PKCdelta and caspases in leukemia cells, *Biochem. Pharmacol* 72 (6) (2006) 681–692. [PubMed: 16844095]
- [38]. DeRose YS, Gligorich KM, Wang G, Georgelas A, Bowman P, Courdy SJ, Welm AL, Welm BE, Patient-derived models of human breast cancer: protocols for in vitro and in vivo applications in tumor biology and translational medicine, *Curr. Protoc. Pharmacol Chapter 14* (2013) Unit14 23.
- [39]. Debnath J, Muthuswamy SK, Brugge JS, Morphogenesis and oncogenesis of MCF-10A mammary epithelial acini grown in three-dimensional basement membrane cultures, *Methods* 30 (3) (2003) 256–268. [PubMed: 12798140]
- [40]. Malavez Y, Voss OH, Gonzalez-Mejia ME, Parihar A, Doseff AI, Distinct contribution of protein kinase Cdelta and protein kinase Cepsilon in the lifespan and immune response of human blood monocyte subpopulations, *Immunology* 144 (4) (2015) 611–620. [PubMed: 25322815]
- [41]. Gyorffy B, Lanczky A, Eklund AC, Denkert C, Budczies J, Li Q, Szallasi Z, An online survival analysis tool to rapidly assess the effect of 22,277 genes on breast cancer prognosis using microarray data of 1,809 patients, *Breast Cancer Res. Treat* 123 (3) (2010) 725–731. [PubMed: 20020197]
- [42]. Weeber F, Ooft SN, Dijkstra KK, Voest EE, Tumor organoids as a pre-clinical cancer model for drug discovery, *Cell Chem. Biol* 24 (9) (2017) 1092–1100. [PubMed: 28757181]
- [43]. Bodmer JL, Holler N, Reynard S, Vinciguerra P, Schneider P, Juo P, Blenis J, Tschopp J, TRAIL receptor-2 signals apoptosis through FADD and caspase-8, *Nat. Cell Biol* 2 (4) (2000) 241–243. [PubMed: 10783243]
- [44]. Li P, Nijhawan D, Budihardjo I, Srinivasula SM, Ahmad M, Alnemri ES, Wang X, Cytochrome c and dATP-dependent formation of Apaf-1/caspase-9 complex initiates an apoptotic protease cascade, *Cell* 91 (4) (1997) 479–489. [PubMed: 9390557]
- [45]. Wu H, Hait WN, Yang JM, Small interfering RNA-induced suppression of MDR1 (P-glycoprotein) restores sensitivity to multidrug-resistant cancer cells, *Cancer Res* 63 (7) (2003) 1515–1519. [PubMed: 12670898]
- [46]. Gyorffy B, Serra V, Jurchott K, Abdul-Ghani R, Garber M, Stein U, Petersen I, Lage H, Dietel M, Schafer R, Prediction of doxorubicin sensitivity in breast tumors based on gene expression profiles of drug-resistant cell lines correlates with patient survival, *Oncogene* 24 (51) (2005) 7542–7551. [PubMed: 16044152]
- [47]. Mahbub AA, Le Maitre CL, Haywood-Small SL, Cross NA, Jordan-Mahy N, Polyphenols act synergistically with doxorubicin and etoposide in leukaemia cell lines, *Cell Death Discov* 1 (2015) 15043. [PubMed: 27551472]
- [48]. Zhao Y, Huan ML, Liu M, Cheng Y, Sun Y, Cui H, Liu DZ, Mei QB, Zhou SY, Doxorubicin and resveratrol co-delivery nanoparticle to overcome doxorubicin resistance, *Sci. Rep* 6 (2016) 35267. [PubMed: 27731405]
- [49]. Gao AM, Ke ZP, Wang JN, Yang JY, Chen SY, Chen H, Apigenin sensitizes doxorubicin-resistant hepatocellular carcinoma BEL-7402/ADM cells to doxorubicin via inhibiting PI3K/Akt/Nrf2 pathway, *Carcinogenesis* 34 (8) (2013) 1806–1814. [PubMed: 23563091]
- [50]. Hong J, Fristiohady A, Nguyen CH, Milovanovic D, Huttary N, Krieger S, Hong J, Geleff S, Birner P, Jager W, Ozmen A, Krenn L, Krupitza G, Apigenin and luteolin attenuate the breaching

of MDA-MB231 breast cancer spheroids through the lymph endothelial barrier in vitro, *Front. Pharmacol* 9 (2018) 220. [PubMed: 29593542]

- [51]. Tsunoda T, Ishikura S, Doi K, Matsuzaki H, Iwaihara Y, Shirasawa S, Resveratrol induces luminal apoptosis of human colorectal cancer HCT116 cells in three-dimensional culture, *Anticancer Res* 34 (8) (2014) 4551–4555. [PubMed: 25075098]
- [52]. Tang S-N, Singh C, Nall D, Meeker D, Shankar S, Srivastava RK, The dietary bioflavonoid quercetin synergizes with epigallocatechin gallate (EGCG) to inhibit prostate cancer stem cell characteristics, invasion, migration and epithelial-mesenchymal transition, *J. Mol. Signal* 5 (2010).
- [53]. Loung CY, Fernando W, Rupasinghe HPV, Hoskin DW, Apple peel flavonoid fraction 4 suppresses breast cancer cell growth by cytostatic and cytotoxic mechanisms, *Molecules* 24 (18) (2019).
- [54]. Liu Y, Hu M, Absorption and metabolism of flavonoids in the caco-2 cell culture model and a perused rat intestinal model, *Drug Metab. Dispos* 30 (4) (2002) 370–377. [PubMed: 11901089]
- [55]. Yu C, Zhang Z, Zhang H, Zhen Z, Calway T, Wang Y, Yuan CS, Wang CZ, Pretreatment of baicalin and wogonoside with glycoside hydrolase: a promising approach to enhance anticancer potential, *Oncol. Rep* 30 (5) (2013) 2411–2418. [PubMed: 24026776]
- [56]. Peterson G, Barnes S, Genistein inhibition of the growth of human breast cancer cells: independence from estrogen receptors and the multi-drug resistance gene, *Biochem. Biophys. Res. Commun* 179 (1) (1991) 661–667. [PubMed: 1883387]
- [57]. Cardenas H, Arango D, Nicholas C, Duarte S, Nuovo GJ, He W, Voss OH, Gonzalez-Mejia ME, Guttridge DC, Grotewold E, Doseff AI, Dietary apigenin exerts immune-regulatory activity in vivo by reducing NF-kappaB activity, halting leukocyte infiltration and restoring normal metabolic function, *Int. J. Mol. Sci* 17 (3) (2016) 323. [PubMed: 26938530]
- [58]. Barros AS, Costa EC, Nunes AS, de Melo-Diogo D, Correia IJ, Comparative study of the therapeutic effect of Doxorubicin and Resveratrol combination on 2D and 3D (spheroids) cell culture models, *Int. J. Pharm* 551 (1–2) (2018) 76–83. [PubMed: 30217766]
- [59]. Maruhashi R, Eguchi H, Akizuki R, Hamada S, Furuta T, Matsunaga T, Endo S, Ichihara K, Ikari A, Chrysin enhances anticancer drug-induced toxicity mediated by the reduction of claudin-1 and 11 expression in a spheroid culture model of lung squamous cell carcinoma cells, *Sci. Rep* 9 (1) (2019) 13753. [PubMed: 31551535]
- [60]. Gao A-M, Zhang X-Y, Ke Z-P, Apigenin sensitizes BEL-7402/ADM cells to doxorubicin through inhibiting miR-101/Nrf2 pathway, *Oncotarget* 8 (47) (2017) 82085–82091. [PubMed: 29137246]
- [61]. Arango D, Parihar A, Villamena FA, Wang L, Freitas MA, Grotewold E, Doseff AI, Apigenin induces DNA damage through the PKC δ -dependent activation of ATM and H2AX causing down-regulation of genes involved in cell cycle control and DNA repair, *Biochem. Pharmacol* 84 (12) (2012) 1571–1580. [PubMed: 22985621]
- [62]. Pilco-Ferreto N, Calaf GM, Influence of doxorubicin on apoptosis and oxidative stress in breast cancer cell lines, *Int. J. Oncol* 49 (2) (2016) 753–762. [PubMed: 27278553]
- [63]. Shukla S, Gupta S, Apigenin: a promising molecule for cancer prevention, *Pharm. Res* 27 (6) (2010) 962–978. [PubMed: 20306120]
- [64]. Golan-Gerstl R, Cohen M, Shilo A, Suh SS, Bakacs A, Coppola L, Karni R, Splicing factor hnRNP A2/B1 regulates tumor suppressor gene splicing and is an oncogenic driver in glioblastoma, *Cancer Res* 71 (13) (2011) 4464–4472. [PubMed: 21586613]
- [65]. Fielding P, Turnbull L, Prime W, Walshaw M, Field JK, Heterogeneous nuclear ribonucleoprotein A2/B1 up-regulation in bronchial lavage specimens: a clinical marker of early lung cancer detection, *Clin. Cancer Res* 5 (12) (1999) 4048–4052. [PubMed: 10632338]
- [66]. Katsimpoula S, Patrinoou-Georgoula M, Makrilia N, Dimakou K, Guialis A, Orfanidou D, Syrigos K, Overexpression of hnRNPA2/B1 in bronchoscopic specimens: a potential early detection marker in lung cancer, *Anticancer Res* 29 (4) (2009) 1373–1382. [PubMed: 19414390]
- [67]. Zhou JM, Jiang H, Yuan T, Zhou GX, Li XB, Wen KM, High hnRNP AB expression is associated with poor prognosis in patients with colorectal cancer, *Oncol. Lett* 18 (6) (2019) 6459–6468. [PubMed: 31819776]

- [68]. Zhou J, Nong L, Wloch M, Cantor A, Mulshine JL, Tockman MS, Expression of early lung cancer detection marker: hnRNP-A2/B1 and its relation to microsatellite alteration in non-small cell lung cancer, *Lung Cancer (Amsterdam, Netherlands)* 34 (3) (2001) 341–350.
- [69]. Liu Y, Li H, Liu F, Gao LB, Han R, Chen C, Ding X, Li S, Lu K, Yang L, Tian HM, Chen BB, Li X, Xu DH, Deng XL, Shi SL, Heterogeneous nuclear ribonucleoprotein A2/B1 is a negative regulator of human breast cancer metastasis by maintaining the balance of multiple genes and pathways, *EBioMedicine* 51 (2020), 102583. [PubMed: 31901866]
- [70]. Krishnamurthy P, Ross DD, Nakanishi T, Bailey-Dell K, Zhou S, Mercer KE, Sarkadi B, Sorrentino BP, Schuetz JD, The stem cell marker Bcrp/ABCG2 enhances hypoxic cell survival through interactions with heme, *J. Biol. Chem* 279 (23) (2004) 24218–24225. [PubMed: 15044468]
- [71]. Soung N-K, Kim H-M, Asami Y, Kim DH, Cho Y, Naik R, Jang Y, Jang K, Han HJ, Ganipiseti SR, Mechanism of the natural product moracin-O derived MO-460 and its targeting protein hnRNPA2B1 on HIF-1 α inhibition, *Exp. Mol. Med* 51 (2) (2019) 1–14.
- [72]. Pradhan M, Bembinster LA, Baumgarten SC, Frasar J, Proinflammatory cytokines enhance estrogen-dependent expression of the multidrug transporter gene ABCG2 through estrogen receptor and NF{ κ }B cooperativity at adjacent response elements, *J. Biol. Chem* 285 (41) (2010) 31100–31106. [PubMed: 20705611]
- [73]. Jin X-Y, Ren C-S, VEGF expression is inhibited by apigenin in human breast cancer cells, *Chin. J. Cancer Res* 18 (4) (2006) 306–311.
- [74]. Seo H-S, Choi H-S, Kim S-R, Choi YK, Woo S-M, Shin I, Woo J-K, Park S-Y, Shin YC, Ko S-K, Apigenin induces apoptosis via extrinsic pathway, inducing p53 and inhibiting STAT3 and NF κ B signaling in HER2-overexpressing breast cancer cells, *Mol. Cell. Biochem* 366 (1–2) (2012) 319–334. [PubMed: 22527937]

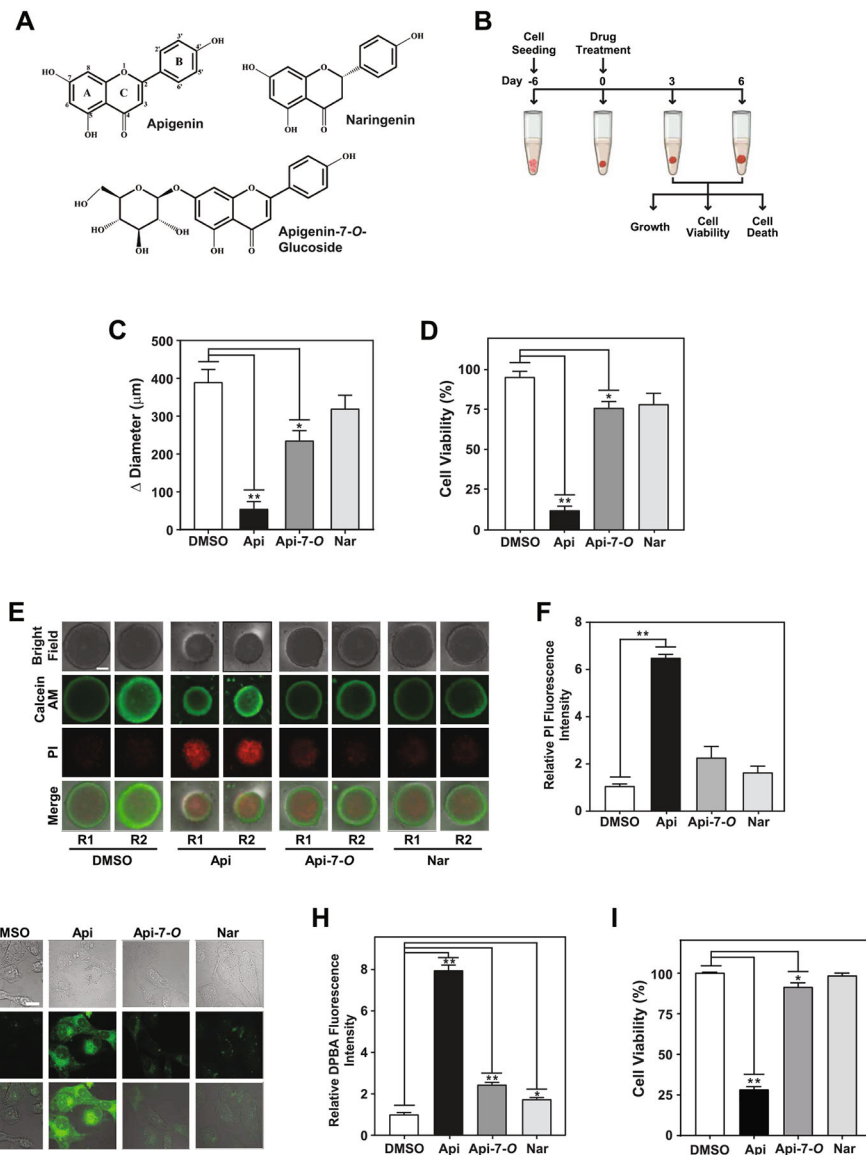


Fig. 1. Apigenin aglycone exhibits greater cytotoxicity than its glycoside in TNBC spheroids. (A) Chemical structure of flavonoids apigenin, naringenin and apigenin-7-*O*-glucoside. (B) Schematic representation of three-dimensional (3D) MDA-MB-231 spheroid formation (from day –6 to 0, corresponding to the time when treatments were initiated) and experimental set-up. Spheroids were treated on day 6 with 50 μM apigenin, apigenin-7-*O*-glucoside, naringenin or DMSO (denoted as 0 in other figures) for 6 days. (C) Spheroid growth represented as diameter between day 6 and day 0. (D) Percentage of cell viability of spheroids treated as indicated in (B) compared with DMSO control. (E) Cell death evaluated by staining spheroids with calcein AM (green) and PI (red) in spheroids treated as indicated in (B). Two representative spheroids, depicted as R1 and R2, shown for each treatment. Scale bar: 250 μm. (F) Relative fluorescence intensity of PI staining from data in (E). Each biological repeat (N) comprised of 3–4 spheroids. (G) Cellular absorption of

flavonoids evaluated by DPBA staining in MDA-MB-231 cells cultured in 2D conditions treated with 50 μ M apigenin, apigenin-7-*O*-glucoside, naringenin, or vehicle DMSO for 48 h and visualized by microscopy. Scale bar: 20 μ m. (H) Relative DPBA fluorescence intensity from data represented in (G). (I) Percentage of cell viability relative to vehicle DMSO in MDA-MB-231 cells treated as in (G). All data represent mean \pm SEM, N = 3, or 5 for (H). * p < 0.05, ** p < 0.001, compared to DMSO control.

Author Manuscript

Author Manuscript

Author Manuscript

Author Manuscript

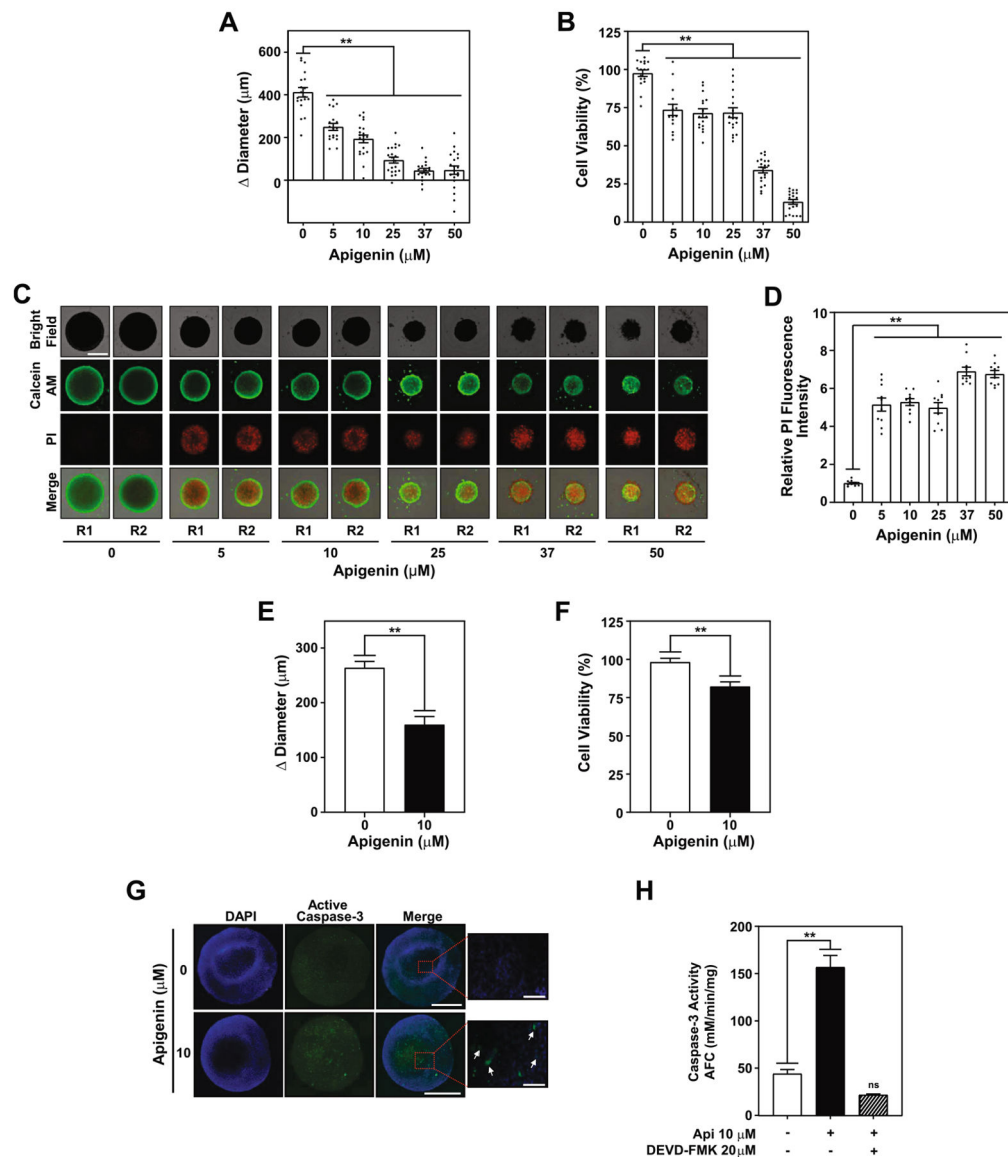


Fig. 2. Apigenin-induced apoptosis in spheroids triggers caspase-3 activity. TNBC MDA-MB-231 spheroids were treated with 5, 10, 25, 37, 50 μM apigenin or DMSO (denoted as 0) for 6 days. (A) Spheroid growth represented as diameter between day 6 and day 0. (B) Percentage of cell viability of spheroids treated as indicated in (A) compared with DMSO control. Data represent mean \pm SEM, $N = 5$; each biological repeat (N) comprised of 3–4 spheroids. (C) Cell death evaluated by staining spheroids with calcein AM (green) and PI (red) in spheroids treated as in (A). Two representative spheroids, R1 and R2, shown for each treatment. Scale bar: 500 μm . (D) Relative fluorescence intensity of PI staining of data shown in (C). Each biological repeat (N) comprised of 3–4 spheroids. (E) Spheroid growth represented as diameter between day 3 and day 0, and (F) percentage of cell viability relative to DMSO, of spheroids treated with 10 μM apigenin for 3 days. Each biological repeat (N) comprised of 4 spheroids. (G) Representative images of spheroids treated with 10

μM apigenin for 3 days immuno-stained with active caspase-3 antibodies (green) and DAPI (blue). Scale bar: 500 μm (20X, 3 panels on left); 100 μm (40X, right panel) (H) Caspase-3 activity was determined in cellular lysates of spheroids pretreated for 2 h with 20 μM DEVD-FMK or DMSO prior to the addition of 10 μM apigenin or DMSO for 3 days. All data represent mean \pm SEM, N = 3. ** $p < 0.001$, compared to DMSO vehicle control; ns indicates no statistical difference.

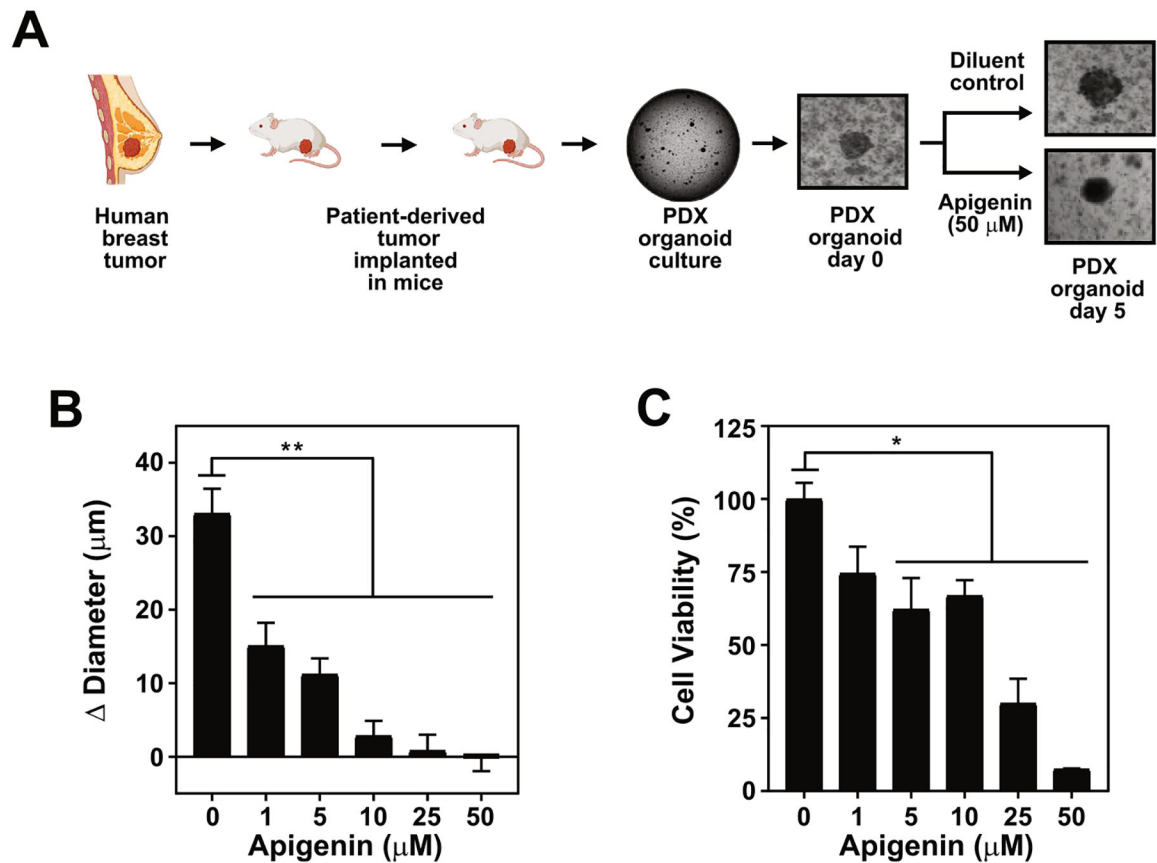


Fig. 3.

Apigenin reduces the viability of human TNBC PDX organoids at concentrations achievable *in vivo*. (A) Schematic representation of organoid formation from human TNBC PDX HCl001 derived from patient-derived xenografts. Organoids were treated with 1, 5, 10, 25, 50 μM apigenin or vehicle DMSO (indicated as 0) for 5 days. (B) Growth represented as diameter between day 5 and day 0 of organoids treated as shown in (A). (C) Percentage of cell viability relative to DMSO in organoids treated as shown in (A). Data represent mean \pm SEM, N = 4; each biological repeat (N) comprised of 10–15 organoids. * $p < 0.05$, ** $p < 0.001$, compared to DMSO vehicle control.

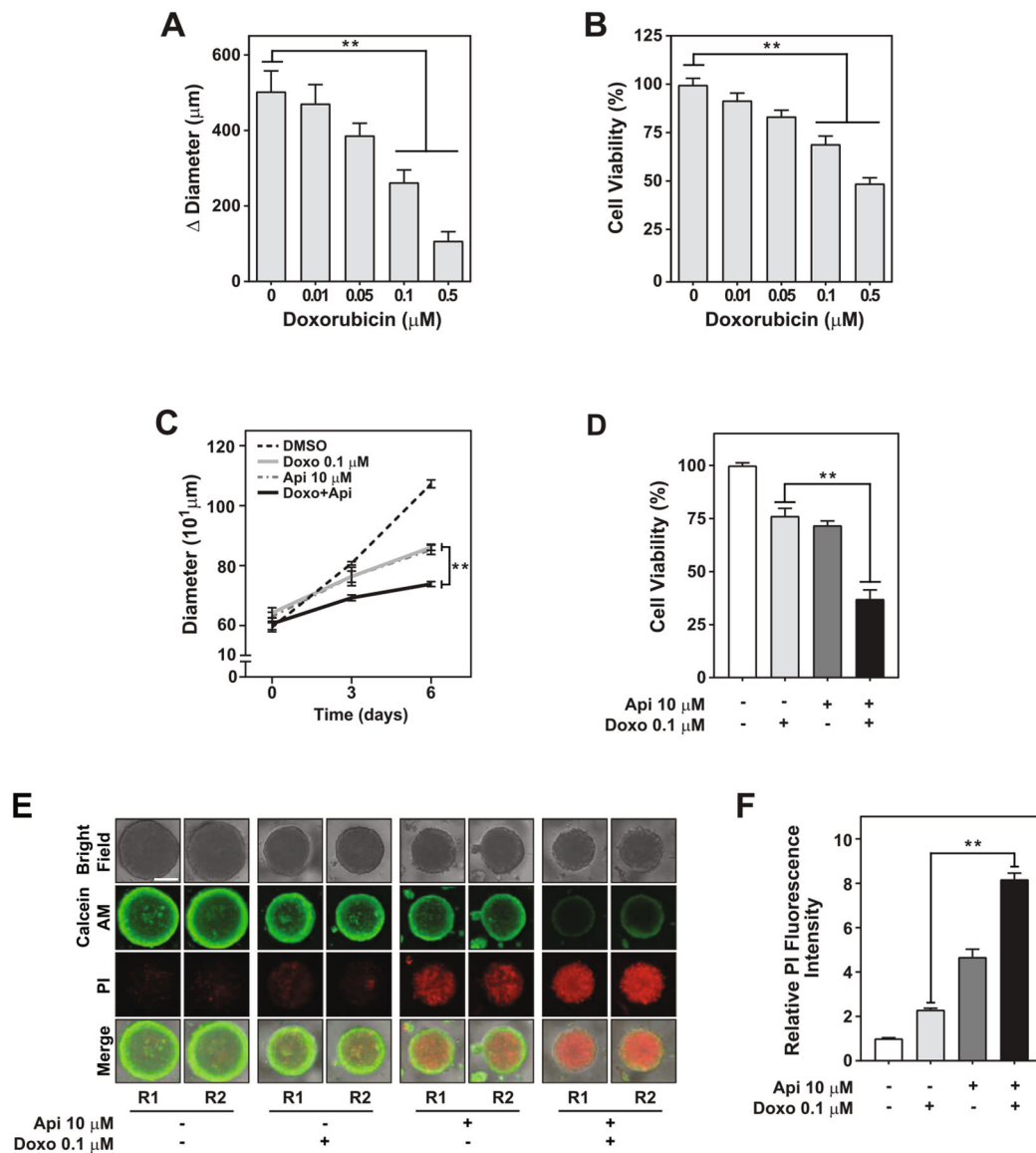


Fig. 4. Apigenin increases the sensitivity of human TNBC spheroids to doxorubicin-induced cell death. Growth and viability were evaluated in TNBC MDA-MB-231 spheroids treated with 0.01, 0.05, 0.1, 0.5 μM doxorubicin or vehicle DMSO (indicated as 0) for 6 days; (–) indicate use of diluent; (A) Growth represented as Δ diameter between day 6 and day 0; (B) Percentage of cell viability relative to DMSO. (C) The growth rate was evaluated by assessing the diameter of MDA-MB-231 spheroids treated with DMSO, 0.1 μM doxorubicin, 10 μM apigenin, or simultaneously with doxorubicin and apigenin at day 3 and day 6. (D) The percentage of cell viability relative to DMSO was evaluated at day 6 in spheroids treated as shown in (D). (E) Cell death evaluated by staining spheroids with calcein AM (green) and PI (red) on day 6 in spheroids treated as shown in (D). Two representative spheroids, depicted as R1 and R2, shown for each treatment. Scale bar: 400 μm . (F) Relative fluorescence intensity of PI staining of data shown in (F). All data represent

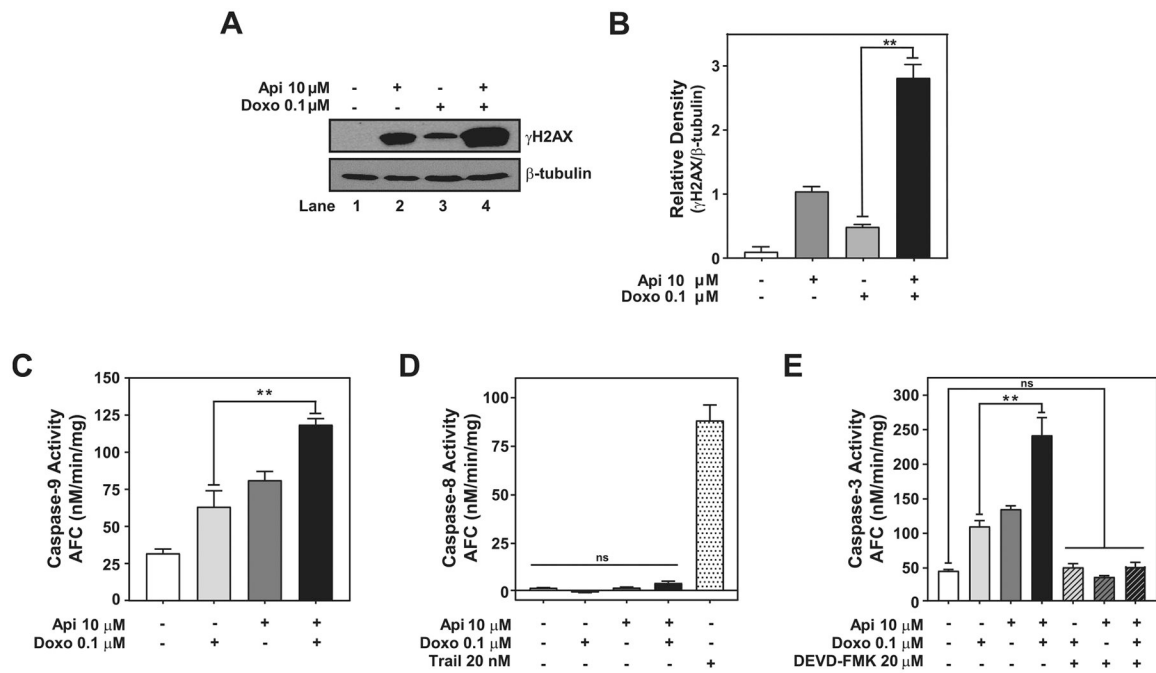
mean \pm SEM, N = 2 or 3; each biological repeat (N) comprised of 2–3 spheroids. ** $p < 0.001$, compared to doxorubicin alone treatment.

Author Manuscript

Author Manuscript

Author Manuscript

Author Manuscript

**Fig. 5.**

Apigenin enhances doxorubicin cytotoxicity by inducing DNA damage and activation of the intrinsic apoptotic pathway. TNBC MDA-MB-231 spheroids treated with DMSO, 0.1 μ M doxorubicin, 10 μ M apigenin or simultaneously with doxorubicin and apigenin for 6 days were used to obtain protein lysates. (A) An equal amount of protein lysates from spheroids were analyzed by western blotting using anti- γ H2AX antibodies. The same membranes were re-blotted with anti- β -tubulin antibodies, used as the loading control. (B) Relative γ H2AX to β -tubulin density of data shown in (A). (C) Protein lysates from spheroids were used to evaluate caspase-9 activity by LEHD-AFC assays. (D) Protein lysates from spheroids were used to evaluate caspase-8 activity by IETD-AFC assays. Protein lysate from spheroids treated with 20 nM TRAIL for 6 days were used as a positive control to evaluate the activation of caspase-8. (E) Caspase-3 activity was evaluated by DEVD-AFC assays in protein lysates from spheroids pretreated for 2 h with DMSO or 20 μ M DEVD-FMK prior to treatment with 0.1 μ M doxorubicin, 10 μ M apigenin or simultaneously with doxorubicin and apigenin for 6 days. Data represent mean \pm SEM, N = 3. ** p < 0.001, compared to single treatment with doxorubicin, ns indicates no statistical difference.

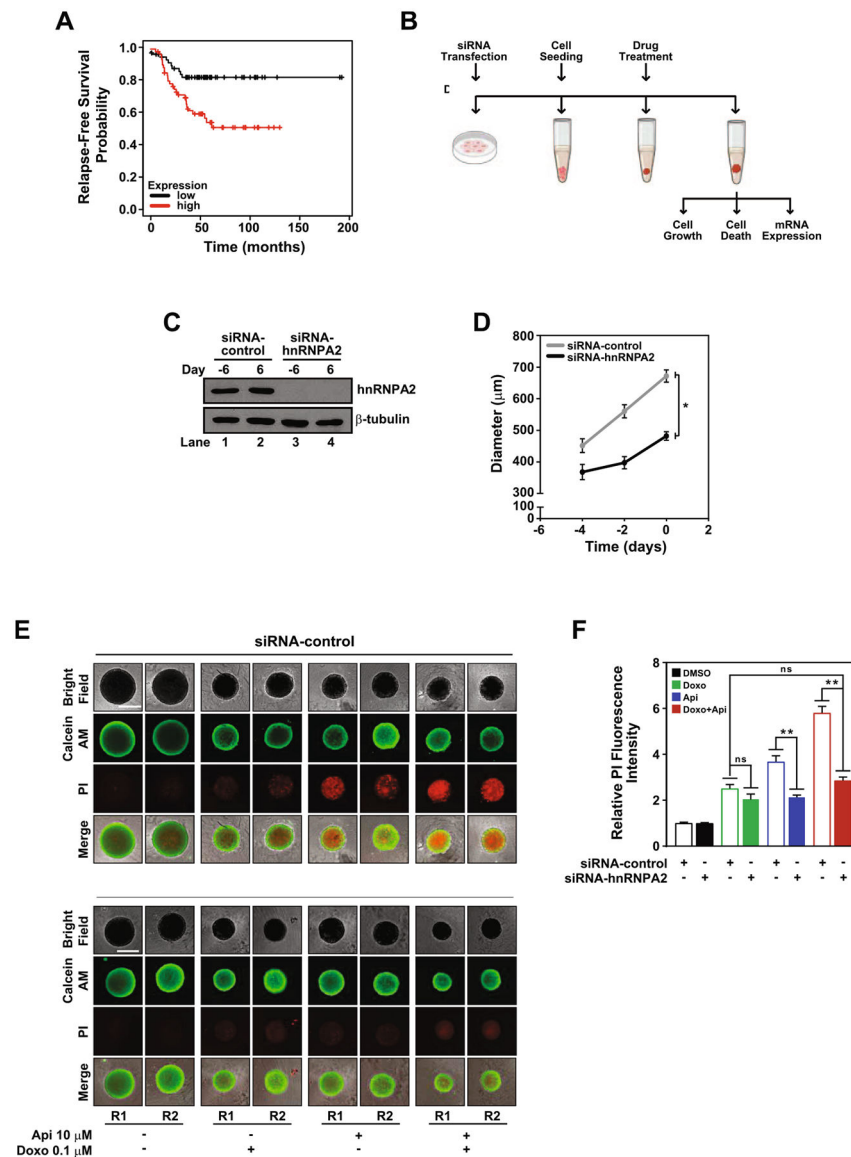


Fig. 6. HnRNPA2 regulates apigenin-mediated sensitization of TNBC spheroids to doxorubicin-induced apoptosis. (A) Kaplan-Meier survival curve was analyzed for hnRNPA2 expression and the probability of Relapse-Free Survival in TNBC patients (log-rank $p = 0.0033$). (B) Schematic representation of experiments involving silencing of hnRNPA2, spheroid formation and treatments. MDA-MB-231 cells cultured in 2D were transfected with siRNA-control or siRNA-hnRNPA2 and used to form spheroids (day -6 to day 0). (C) hnRNPA2 protein expression was evaluated by western blotting of protein lysates of siRNA-control or siRNA-hnRNPA2 silenced cells (lanes 1 and 3) collected at day -6 and spheroids (lanes 2 and 4) at day 6, equal amounts of protein lysates loaded and membranes immunoblotted with anti-hnRNPA2 antibodies. The same membranes were re-blotted with anti- β -tubulin antibodies. (D) Growth curve of siRNA-control or siRNA-hnRNPA2 silenced spheroids. (E) Cell death evaluated by calcein AM (green) and PI (red) staining in siRNA-hnRNPA2 and

siRNA-control spheroids treated with DMSO, 0.1 μ M doxorubicin, 10 μ M apigenin or simultaneously with doxorubicin and apigenin in combination for 6 days. Two representative spheroids, depicted as R1 and R2, shown for each treatment. Scale bar: 500 μ m. (F) Relative fluorescence intensity of PI staining from samples shown in (D). Data represent mean \pm SEM, N = 3; each biological repeat (N) comprised of 3–4 spheroids. * p < 0.015, ** p < 0.001, compared to siRNA-control subjected to similar treatment, ns indicates no statistical difference among indicated treatments.

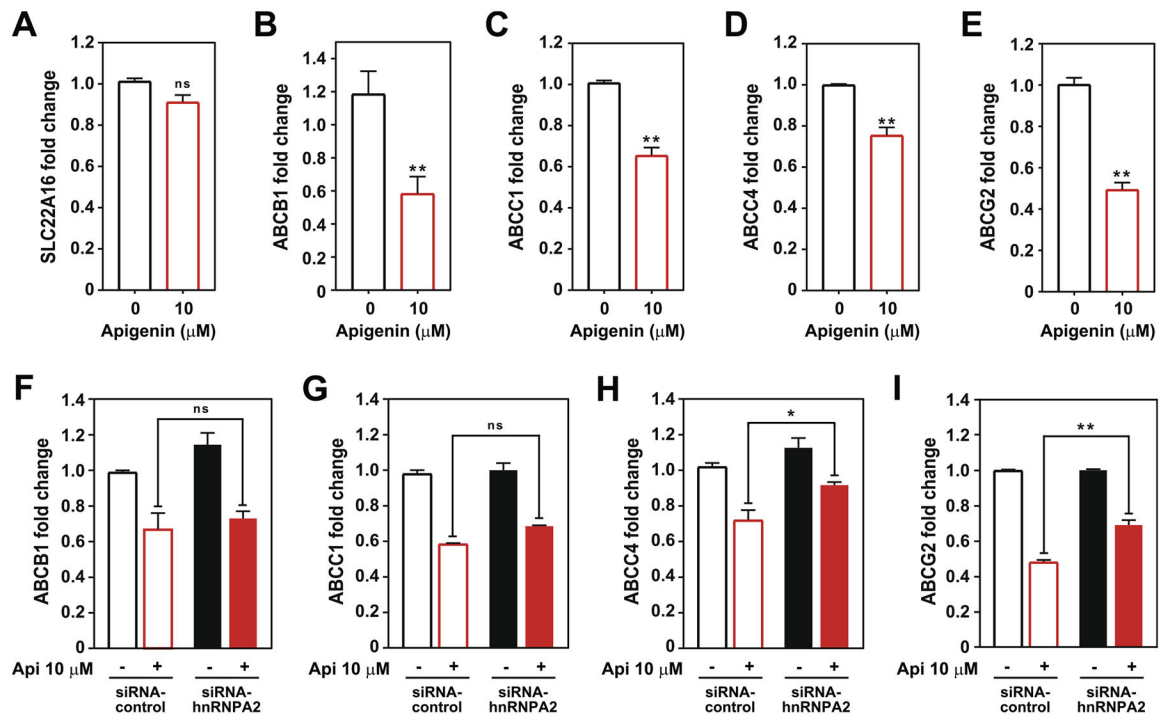


Fig. 7.

Apigenin reduces the expression of doxorubicin efflux transporters through hnRNPA2-dependent and independent mechanisms. Steady state mRNA levels of (A) *SLC22A16*, (B) *ABCB1*, (C) *ABCC1*, (D) *ABCC4* and (E) *ABCG2* in TNBC MDA-MB-231 spheroids treated with 10 μM apigenin or vehicle DMSO for 6 days and analyzed using qRT-PCR. Data represent mean ± SEM, N = 3. ** $p < 0.001$, compared to DMSO control (indicated as 0). Steady state mRNA levels of (F) *ABCB1*, (G) *ABCC1*, (H) *ABCC4* and (I) *ABCG2* in siRNA-control (empty bars) and siRNA-hnRNPA2 silenced spheroids (solid bars) treated with 10 μM apigenin or DMSO (indicated as -) for 6 days and analyzed using qRT-PCR. Data represent mean ± SEM, N = 3. * $p < 0.05$, ** $p < 0.001$; compared to siRNA-control subjected to similar treatment, ns indicates no statistical difference among indicated treatments.

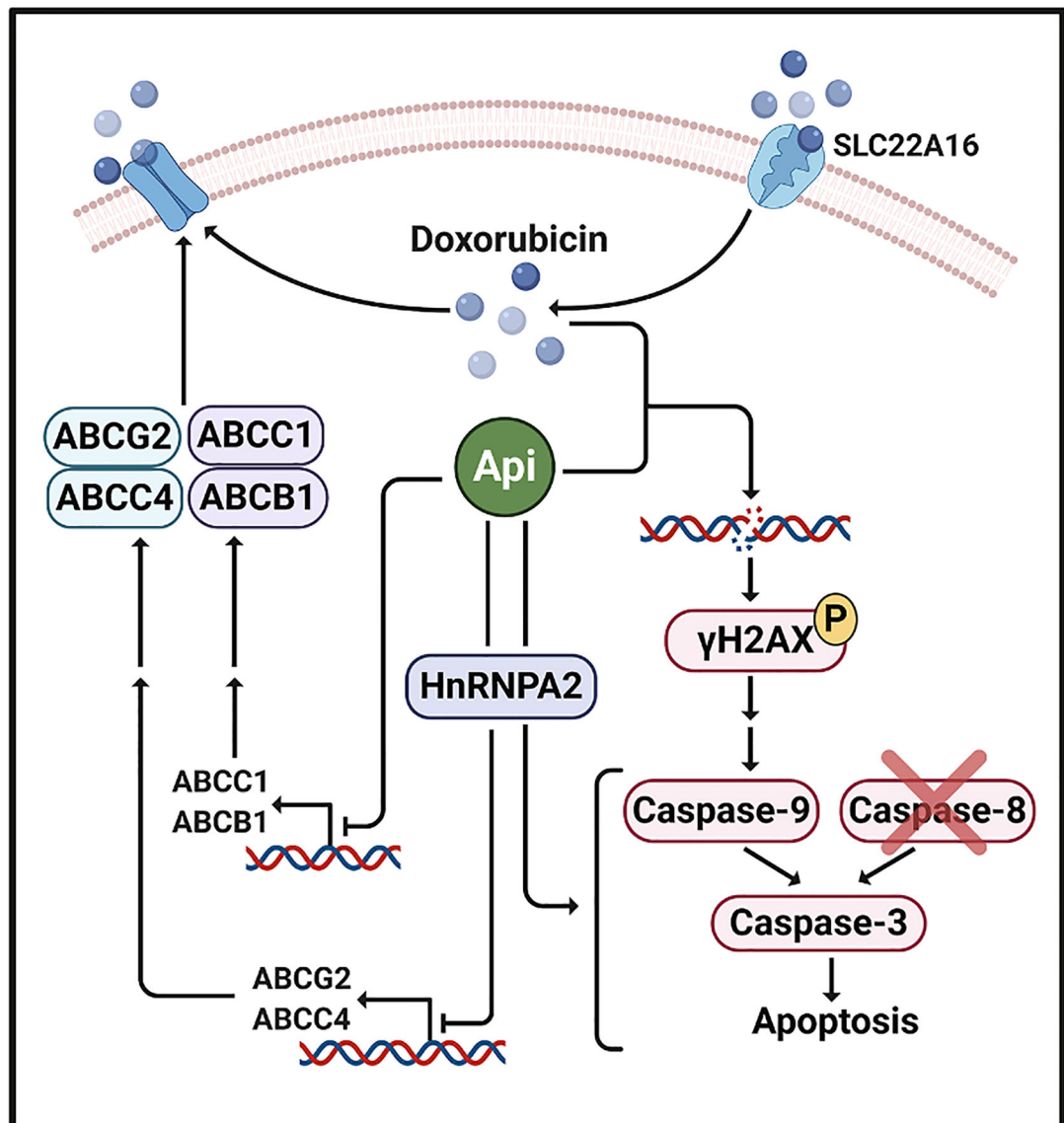


Fig. 8. Schematic model of molecular mechanisms involved in apigenin-induced sensitization to doxorubicin in human TNBC spheroids. Apigenin sensitizes TNBC spheroids to doxorubicin treatment by inducing double stranded DNA breaks and triggering the caspase-9-mediated intrinsic apoptotic pathway leading to caspase-3 activation, without impacting caspase-8 activity. Thus, apigenin through hnRNPA2 sensitizes TNBC spheroids to doxorubicin-induced apoptosis. In addition, through hnRNPA2 dependent and independent mechanisms apigenin downregulates the expression of ABC efflux transporters, which may lead to increased doxorubicin accumulation.